

APPROXIMATION METHODS IN FIBER OPTICS

By

TRI VAN

A DISSERTATION PRESENTED TO THE GRADUATE SCHOOL
OF THE UNIVERSITY OF FLORIDA IN PARTIAL FULFILLMENT
OF THE REQUIREMENTS FOR THE DEGREE OF
DOCTOR OF PHILOSOPHY

UNIVERSITY OF FLORIDA

1999

To my parents

ACKNOWLEDGEMENTS

First and foremost, I would like to thank my advisor, Dr. Gang Bao, for his constant guidance and encouragement. His wisdom profoundly influences me.

I would also like to thank Dr. Lawrence Cowsar from Lucent Technologies for being my mentor during my internship at the company, Dr. William Hager for his finite element class, Dr. Li-Chien Shen for his generosity, and Dr. Weihong Tan for his service on my supervisory committee.

I wish to thank Dr. J. Allen Cox from Honeywell Inc. who taught me fiber optics.

I am especially grateful to my parents, my brother, Ton, and my sister, Tien.

TABLE OF CONTENTS

ACKNOWLEDGEMENTS	iii
ABSTRACT	vi
CHAPTERS	
1 INTRODUCTION	1
2 WEAKLY-GUIDING APPROXIMATION	5
2.1 Circular Optical Fibers	5
2.2 Time Harmonic Maxwell's Equations and Transmission Conditions	6
2.3 Weakly-Guiding Approximation	8
3 PERTURBATION OF GUIDED MODES IN CIRCULAR FIBERS	16
3.1 Eigenvalue Approximations	16
3.2 Scalar Wave Equation E_z	28
3.3 Perturbed Fibers	30
3.4 Truncated Parabolic Profile	31
3.5 Distortions	33
3.6 Frequency Response and Bandwidth	34
3.7 Numerical Experiments	35
3.7.1 First Order and Second Order Approximations	35
3.7.2 Bandwidths of Perturbed Fibers	36
4 A FINITE ELEMENT METHOD FOR CIRCULAR FIBERS	44
4.1 Unbounded Domain or Non-Compact Problem	44
4.2 Variational Formulation for E_z Field	46
4.3 Finite Element Approximations	51
4.4 Convergence of Eigenvalues and Eigenfunctions	55
4.5 The Subspaces V_h	57
4.6 Numerical Experiments	64

5	NON-CIRCULAR FIBERS AND DTN MAPS	71
5.1	Dirichlet-to-Neumann Map	71
5.2	Variational Formulation of Interior Problem	78
5.3	Finite Element Approximation	81
5.4	Numerical Experiments	84
5.5	Square Fiber Versus Circular Fiber	86
	REFERENCES	95
	BIOGRAPHICAL SKETCH	98

Abstract of Dissertation Presented to the Graduate School
of the University of Florida in Partial Fulfillment of the
Requirements for the Degree of Doctor of Philosophy

APPROXIMATION METHODS IN FIBER OPTICS

By

Tri Van

August 1999

Chairman: Dr. Gang Bao
Major Department: Mathematics

* Perturbation methods were used to study the propagating fields inside a weakly-guiding circular fiber whose refractive index profile is slightly deviated from the optimal truncated-parabolic shape. It was observed that the performance of the fiber is reduced dramatically. Next, finite element methods are considered to solve Sturm-Liouville and Helmholtz equations defined in unbounded domains so that the non-physical solutions can be eliminated from the computations. It is known that a circular fiber with a smaller core yields more evanescent energy. From numerical results, it was observed that a step-index square fiber whose core cross-sectional area is slightly larger than that of a step-index circular fiber still has more evanescent energy than the circular fiber.

CHAPTER 1 INTRODUCTION

Optical fibers have many important applications in telecommunications, evanescent wave sensing and image processing. There is a vast amount of research papers and books in electrical engineering and applied mathematics devoted to the study of their properties and performance. In this work, we present some of the approximation methods that are useful in estimating the propagating electromagnetic fields in circular and non-circular fibers.

In telecommunications, circular weakly-guiding fibers are used to transmit information of several hundred Mbits/sec. They are characterized by the small difference in the core and cladding refractive indices. In this case, Maxwell's equations can be well approximated by Helmholtz equations by ignoring the polarization effect (or first-order approximation). These equations can be further reduced to Sturm-Liouville equations using polar coordinates. This simplification is possible due to the circular symmetry of the fibers. It has been shown that multi-mode fibers with a truncated parabolic refractive index profile achieve the optimum bandwidth-the information carrying capacity [5]. In the process of fiber fabrication, however, it is not possible to obtain the exact parabolic shape for the refractive index profile. Therefore, it is of importance to examine the effect on the fiber bandwidth when its index profile is slightly deviated from the ideal shape. Perturbation methods are often used for this type of problem. It is known that a small perturbation to the optimal profile reduces the fiber bandwidth dramatically [30, 15, 24, 25]. This negative effect can be

predicted by calculating the Fourier transform of the impulse response of the fiber which is defined in terms of propagation constants β . At the present, many fiber manufacturers still use the first order perturbation method developed by Olshansky [30]. In this method, the transverse electric field for the optimal profile is approximated by the Laguerre solution for the wave guide with *infinite* parabolic profile and the study of field perturbation is carried out in terms of the Laguerre functions. Marcuse *et al* later presented a different approach to the same problem using WKB approximation [24, 25]. However, this method is known to fail at turning points. We will present a better approximation using first and second order perturbation methods based on the exact analytical solutions (eigenvalues and eigenfunctions) of the optimal profile. These exact solutions can be expressed in terms of Whittaker functions of the first kind and modified Bessel functions [32, 34]. We also give the estimates for the coefficients of the Taylor expansion of the perturbed eigenvalues.

For arbitrary index profile shape, we rely on finite element methods to find the solutions of singular Sturm-Liouville equations. The singularity arises from the unboundedness of the considered domain. As a result, weighted Sobolev spaces and modified finite element spaces are needed. In this case, the usual finite dimensional approximating spaces are replaced by infinite dimensional spaces to reduce the computational domain and to eliminate non-physical solutions called spurious modes. This technique is discussed in [17] where an unbounded interval is reduced a bounded one, I , on which the usual finite element functions are used (*e.g.*, piecewise linear functions). Outside of I , all H^1 functions with compact support in $\mathbb{R} \setminus I$ will be contained in the approximate subspaces. This method yields the same convergence rates for eigenfunctions and eigenvalues as in the standard bounded interval case, *i.e.*, the order of the eigenvalue error is the square of the order of the interpolation error if the

eigenfunctions are sufficiently smooth. To use this method, however, one has to have the fundamental solutions at each end of the bounded interval I as boundary functions. In our problem, only the fundamental solution at infinity is available. Thus, it is natural to generalize this method by using appropriate approximating subspaces. We also obtain the same convergence rates for eigenvalues and eigenfunctions.

If the core of the fiber is not circular but rather rectangular or of any other shape, Helmholtz or Maxwell's equations have to be solved. A numerical method developed in [16] uses the circular harmonic series representation of the electromagnetic fields in rectangular fibers, *i.e.*, the series of Bessel and modified Bessel functions. Though one can obtain a solution as accurate as desired by increasing the number of terms in the series expansion, the computation is complicated and costly. A more attractive alternative method is given in [23]. In this method, the exterior corner regions of a rectangular waveguide is completely ignored. This approximation is justified only when the mode is not very close to cut-off. However, in fiber optic sensor application, the modes near cut-off play an important role since a large fraction of their energy leaks into the exterior region which can be used for chemical detection. Thus, finite element methods again become the obvious choice for solving the problem numerically. The electromagnetic fields of guided modes in a fiber satisfy Helmholtz equations in the whole \mathbb{R}^2 . Since the domain is unbounded, it is custom to impose the zero Dirichlet condition $u = 0$ on an artificial boundary sufficiently far away from the fiber core. This method is justified by the exponentially decaying property of guided modes outside the core. The portions of guided modes that exists in the cladding is called evanescent waves. They have applications in spectroscopy and fiber optic evanescent sensing. Unfortunately, this standard method is known to have many spurious (non-physical) solutions. This phenomenon has been observed and

studied by, for example, Rappaz in [31]. To eliminate these spurious solutions, we borrow a technique known as Dirichlet-to-Neumann maps (DtN maps) developed for exterior and scattering problems. This technique introduces an artificial boundary and imposes on it a relationship (map) between Dirichlet and Neumann boundary conditions. A good reference to this useful method is [14]. The Dirichlet-to-Neumann maps can be applied successfully to our unbounded problem. It also turns out that the error estimates are easily proved using the positive definite property of DtN maps and a trace theorem. We apply this method to calculate and compare the evanescent energy of a step-index square fiber and that of a step-index circular fiber. This energy existing outside of the core of a fiber is useful in optical spectroscopy. For numerical experiments, we choose a step-index square fiber with a slightly larger cross-section area than the cross-section area of a step-index circular fiber. This choice is justified by the fact that in general a fiber with a smaller core has more evanescent energy. In spite of having the larger core, the square fiber is observed to have more evanescent energy existing outside of the core than the circular fiber.

CHAPTER 2 WEAKLY-GUIDING APPROXIMATION

2.1 Circular Optical Fibers

An optical fiber is a three dimensional cylindrical medium consisting of two major parts: the inner core made of dielectric material like silica or composite material of different refractive indices (graded fibers) and the outer cladding surrounding the core, usually made of a lower refractive index material like plastic or silica non-doped. The cladding is considered to be extended to infinity in the radial direction for purposes of analysis. This assumption is justified in practice where the cladding is much larger than the core in diameter. We orient the fiber so that its longitudinal axis is parallel to the z -axis in \mathbb{R}^3 . We also assume that the geometry of the transverse cross-section and refractive index distribution of the fiber are z -translationally invariant, *i.e.*,

$$n(x, y, z) = n(x, y), \quad (x, y) \in \mathbb{R}^2.$$

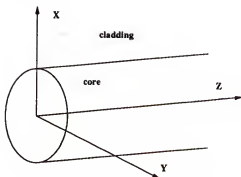


Figure 2.1: Optical fiber

Let $\Omega \times \mathbb{R}$ denote the core region where Ω is the two dimensional transverse cross section. Denote

$$\begin{aligned} n_{co} &= \max_{(x,y) \in \Omega} n(x,y), \\ n_{cl} &= \text{cladding index.} \end{aligned} \quad (2.1)$$

In order for a guidance to take place in a fiber, the guiding condition must be satisfied, i.e.,

$$n_{co} > n_{cl}. \quad (2.2)$$

Definition 2.1.1 *The normalized index difference Δ is defined as*

$$\Delta = \frac{1}{2} \frac{n_{co}^2 - n_{cl}^2}{n_{co}^2}. \quad (2.3)$$

This parameter is important in fiber optics. There are two major classes of commercial fibers: multi-mode and single-mode. A single-mode fiber allows one propagating mode while a multi-mode fiber has more than one propagating mode. A multi-mode fiber usually has the core radius between 25 and 50 μm and the normalized index difference $\Delta \approx 1\%$. A single-mode has the core radius between 2 and 5 μm and the normalized index difference $\Delta \approx 0.2\%$. The standardized measurement for the cladding diameter is 125 μm .

The electromagnetic fields in a fiber are governed by Maxwell's equations.

2.2 Time Harmonic Maxwell's Equations and Transmission Conditions

The general Maxwell equations for electromagnetic fields

$(\underline{\mathbb{E}}(x, y, z, t), \underline{\mathbb{H}}(x, y, z, t))$ are

$$\begin{cases} \epsilon \frac{\partial \underline{\mathbb{E}}}{\partial t} - \nabla \times \underline{\mathbb{H}} = 0, \\ \mu_0 \frac{\partial \underline{\mathbb{H}}}{\partial t} + \nabla \times \underline{\mathbb{E}} = 0. \end{cases} \quad (2.4)$$

where μ_0 is the free-space magnetic permeability, $\varepsilon(x, y, z) = \varepsilon_0 n^2(x, y, z)$ is the electric permittivity of the medium, ε_0 is the free-space electric permittivity, and n is the refractive index distribution of the material. In our treatment, waves are assumed to propagate in linear media, that is, ε is independent of field strength.

For a time harmonic wave, its electromagnetic fields are expressed as

$$\begin{aligned}\underline{\mathbb{E}}(x, y, z, t) &= \mathbb{E}(x, y, z)e^{-i\omega t}, \\ \underline{\mathbb{H}}(x, y, z, t) &= \mathbb{H}(x, y, z)e^{-i\omega t}.\end{aligned}\tag{2.5}$$

where ω is the angular frequency. Let c be the speed of light in free space, then $c = (\varepsilon_0\mu_0)^{-1/2}$ and $k = \frac{\omega}{c} = \frac{2\pi}{\lambda}$ is the wave number.

Time harmonic Maxwell's equations are of the form

$$\left\{ \begin{array}{l} \nabla \times \mathbb{E} = i\omega\mu_0\mathbb{H}, \\ \nabla \times \mathbb{H} = -i\omega\varepsilon\mathbb{E}, \\ \nabla \cdot (\varepsilon\mathbb{E}) = 0, \\ \nabla \cdot \mathbb{H} = 0. \end{array} \right.\tag{2.6}$$

Transmission conditions. When the electromagnetic field crosses a surface S which is a boundary of two distinct media of different refractive indices, it is necessary to impose the following conditions known as *transmission conditions*. Let \hat{n} denote the normal unit vector to S pointing from, say, medium 1 to medium 2. Let $\mathbb{E}^{(i)}, \mathbb{H}^{(i)}, i = 1, 2$, be the electromagnetic field in the medium $i, i = 1, 2$. Then on S we impose the following:

$$\mathbb{E}^{(1)} \times \hat{n} = \mathbb{E}^{(2)} \times \hat{n},\tag{2.7}$$

$$\mathbb{H}^{(1)} \times \hat{n} = \mathbb{H}^{(2)} \times \hat{n},\tag{2.8}$$

$$n_1^2 \mathbb{E}^{(1)} \cdot \hat{n} = n_2^2 \mathbb{E}^{(2)} \cdot \hat{n},\tag{2.9}$$

$$\mathbb{H}^{(1)} \cdot \hat{n} = \mathbb{H}^{(2)} \cdot \hat{n},\tag{2.10}$$

where n_1 and n_2 are the refractive indices of medium 1 and medium 2, respectively. In the case of optical fibers, the surface S is usually a circular cylinder and the unit normal vector $\hat{n} = (n_x, n_y, 0)$.

Definition 2.2.1 *A guided wave is a particular solution (\mathbb{E}, \mathbb{H}) to time harmonic Maxwell's equations (or just Maxwell's equations) such that \mathbb{E} and \mathbb{H} satisfy the transmission conditions (2.7-2.10), of the form*

$$\mathbb{E} = E(x, y)e^{-i\beta z},$$

$$\mathbb{H} = H(x, y)e^{-i\beta z},$$

where $E \in [L^2(\mathbb{R}^2)]^3$ and $H \in [L^2(\mathbb{R}^2)]^3$, i.e.,

$$\int_{\mathbb{R}^2} (|E|^2 + |H|^2) \, dxdy < \infty,$$

where $\beta > 0$ is the propagation constant and $kn_{cl} < \beta \leq kn_{co}$.

The definition of guided waves signifies the fact that these waves are plane waves propagating without any distortion in the fiber axis direction (z -direction). The vector-valued two dimensional vector fields $E(x, y) = (E_x(x, y), E_y(x, y), E_z(x, y))$ and $H(x, y) = (H_x(x, y), H_y(x, y), H_z(x, y))$ describe the the distribution of electromagnetic field in each cross-section.

2.3 Weakly-Guiding Approximation

Most of commercial optical fibers used in telecommunications are of weakly guiding type, i.e., the normalized index difference Δ is very small. Consequently, Maxwell's equations can be well approximated by a simpler set of 2D scalar wave equations known as Helmholtz equations. These equations can be further simplified to 1D equations if the geometry of the cross-section is a circular disk. In this section,

we derive the Helmholtz equations. The 1D equations will be addressed in the next chapter. We first return to Maxwell's equations (2.6). From the first two equations we can eliminate, for example, the vector field \mathbf{H} to obtain an equation for \mathbf{E} only, *i.e.*,

$$\nabla \times \nabla \mathbf{E} = \omega^2 \mu_0 \varepsilon \mathbf{E} = k^2 n^2 \mathbf{E}. \quad (2.11)$$

Using the vector identities

$$\begin{aligned} \nabla \times \nabla \cdot \mathcal{F} &= \nabla^2 \mathcal{F} - \nabla(\nabla \cdot \mathcal{F}), \\ \nabla \times (g\mathcal{F}) &= g\nabla \cdot \mathcal{F} + \mathcal{F} \cdot \nabla g, \end{aligned}$$

where \mathcal{F} is a vector-valued function and g a scalar function, we have in each region with smooth n^2 that

$$\begin{aligned} \nabla^2 \mathbf{E} + k^2 n^2 \mathbf{E} &= \nabla(\nabla \cdot \mathbf{E}) \\ &= \nabla(-\mathbf{E} \cdot \frac{\nabla n^2}{n^2}) \\ &= -\nabla(\mathbf{E}_t \cdot \nabla_t \ln(n^2)), \end{aligned} \quad (2.12)$$

where $\mathbf{E}_t := \mathbf{E}_t e^{-i\beta z} := (E_x, E_y)e^{-i\beta z}$ is the transverse component of \mathbf{E} and $\nabla_t := (\frac{\partial}{\partial x}, \frac{\partial}{\partial y})$ is the transverse component of the differential operator ∇ .

Since $\mathbf{E} := (\mathbf{E}_t, E_z)e^{-i\beta z}$, we can also write (2.12) as

$$(\nabla_t^2 + k^2 n^2 - \beta^2)\mathbf{E} = -(\nabla_t - i\beta \hat{z})(\mathbf{E}_t \cdot \nabla_t \ln(n^2)), \quad (2.13)$$

where $\hat{z} = (0, 0, 1)$ is the unit vector in z -direction. Then the equation for the transverse component of \mathbf{E} is

$$(\nabla_t^2 + k^2 n^2 - \beta^2)\mathbf{E}_t = -\nabla_t(\mathbf{E}_t \cdot \nabla_t \ln(n^2)). \quad (2.14)$$

The term $\nabla_t \ln(n^2)$ represents the *polarization effect* that exists when n^2 is a non-constant function. It is convenient to express $n^2(x, y)$ as

$$n^2(x, y) = n_{co}^2(1 - 2\Delta f(x, y)), \quad f(x, y) \geq 0. \quad (2.15)$$

We then expand n^2 in Taylor series in terms of Δ and obtain

$$\begin{aligned} \nabla_t \ln(n^2) &= \nabla_t \ln(1 - 2\Delta f(x, y)) \\ &= \nabla_t(-2\Delta f(x, y) - 2\Delta^2 f^2(x, y) \dots) \\ &= -2\Delta \nabla_t f(x, y) - 2\Delta^2 \nabla_t f^2(x, y) - \dots \end{aligned}$$

If $\Delta \ll 1$, the first-order approximation of (2.14) is

$$(\nabla_t^2 + k^2 n^2 - \beta^2) \mathbb{E}_t = 0. \quad (2.16)$$

This approximation is equivalent to ignoring the polarization effect and is known as *weakly-guiding approximation*. The equation (2.16) is known as a *Helmholtz equation*.

Definition 2.3.1 Assume $\Delta \ll 1$. The weakly-guiding approximation of (time harmonic) Maxwell's equations in terms of \mathbb{E}_t is of the form

$$(\nabla_t^2 + k^2 n^2 - \beta^2) \mathbb{E}_t = 0,$$

or equivalently,

$$(\nabla_t^2 + k^2 n^2 - \beta^2) E_t = 0$$

(the factor $e^{-i\beta z}$ is omitted).

In a similar fashion, we can derive the weakly-guiding approximation for \mathbb{H} . From the first two equations in (2.6) we have

$$\nabla \times \left(\frac{1}{\epsilon} \nabla \times \mathbb{H} \right) = \omega^2 \mu \mathbb{H}. \quad (2.17)$$

Using the vector identity

$$\nabla \cdot (g\mathcal{F}) = g\nabla \times \mathcal{F} + \nabla g \cdot \mathcal{F},$$

we obtain

$$\frac{1}{n^2} \nabla \times \nabla \times \mathbb{H} - \nabla(1/n^2) \times \mathbb{H} = k^2 \mathbb{H},$$

thus, the transverse component of \mathbb{H} satisfies

$$(\nabla_t^2 + k^2 n^2 - \beta^2) \mathbb{H}_t = \nabla_t \ln(n^2) \times \mathbb{H}. \quad (2.18)$$

Hence, the weakly-guiding approximation yields

$$(\nabla_t^2 + k^2 n^2 - \beta^2) \mathbb{H}_t = 0. \quad (2.19)$$

Definition 2.3.2 Assume $\Delta \ll 1$. The weakly-guiding approximation of Maxwell's equations in terms of \mathbb{H}_t is of the form

$$(\nabla_t^2 + k^2 n^2 - \beta^2) \mathbb{H}_t = 0,$$

or equivalently,

$$(\nabla_t^2 + k^2 n^2 - \beta^2) H_t = 0$$

($e^{i\beta z}$ is omitted).

The longitudinal components E_z and H_z of E and H respectively can also be shown to satisfy the scalar Helmholtz equation under the weakly guiding approximation. By writing out the equations $\nabla \times \mathbb{E} = i\omega\mu_0 \mathbb{H}$ and $\nabla \times \mathbb{H} = -i\omega\varepsilon \mathbb{E}$ we get a system of six equations:

$$\begin{aligned} \frac{\partial E_x}{\partial y} + i\beta E_y &= i\omega\mu_0 H_x, \\ -i\beta E_x - \frac{\partial E_z}{\partial x} &= i\omega\mu_0 H_y, \end{aligned}$$

$$\begin{aligned}
\frac{\partial E_y}{\partial x} - \frac{\partial E_x}{\partial y} &= i\omega\mu_0 H_z, \\
\frac{\partial H_z}{\partial y} + i\beta H_y &= -i\omega\varepsilon E_x, \\
-i\beta H_x - \frac{\partial H_z}{\partial x} &= -i\omega\varepsilon E_y, \\
\frac{\partial H_y}{\partial x} - \frac{\partial H_x}{\partial y} &= -i\omega\varepsilon E_z.
\end{aligned}$$

From these equations, we can solve for E_x , E_y , H_x , H_y in terms of the longitudinal components E_z , H_z and their partial derivatives, i.e.,

$$\begin{aligned}
E_x &= \frac{i}{k^2 n^2 - \beta^2} (\beta \frac{\partial E_z}{\partial x} + \omega\mu_0 \frac{\partial H_z}{\partial y}), \\
E_y &= \frac{i}{k^2 n^2 - \beta^2} (\beta \frac{\partial E_z}{\partial y} - \omega\mu_0 \frac{\partial H_z}{\partial x}), \\
H_x &= \frac{i}{k^2 n^2 - \beta^2} (\beta \frac{\partial H_z}{\partial x} - \omega\varepsilon_0 n^2 \frac{\partial E_z}{\partial y}), \\
H_y &= \frac{i}{k^2 n^2 - \beta^2} (\beta \frac{\partial H_z}{\partial y} + \omega\varepsilon_0 n^2 \mu_0 \frac{\partial E_z}{\partial x}).
\end{aligned}$$

Remark: If we set

$$E = (E_x, E_y, -iE_z),$$

$$H = (H_x, H_y, iH_z),$$

then this modification will allow us to work in the real space \mathbb{R}^3 instead of \mathbb{C}^3 .

Thus, it is enough to solve for the longitudinal components E_z and H_z of E and H respectively. The z -component of $\nabla \times \nabla \times \mathbb{E} = k^2 n^2 \mathbb{E}$ satisfies

$$\nabla_t^2 E_z + (k^2 n^2 - \beta^2) E_z = -i\beta E_t \nabla \ln\left(\frac{1}{n^2}\right) \quad (2.20)$$

$$= i\beta E_t \nabla \ln(n^2), \quad (2.21)$$

and the z -component of $\nabla \times (\frac{1}{n^2}) \nabla \times \mathbb{H} = k^2 \mathbb{H}$ satisfies

$$\nabla_t^2 H_z + (k^2 n^2 - \beta^2) H_z = -(\nabla H_z - i\beta H_t) \nabla \ln(n^2). \quad (2.22)$$

As before, if we ignore the polarization effect, we obtain the scalar Helmholtz equations for E_z and H_z :

$$\nabla_t^2 E_z + (k^2 n^2 - \beta^2) E_z = 0, \quad (2.23)$$

$$\nabla_t^2 H_z + (k^2 n^2 - \beta^2) H_z = 0. \quad (2.24)$$

Boundary conditions for scalar Helmholtz equations. Let $\Omega \subset \mathbb{R}^2$ denote the transverse cross-section of the fiber, and $\partial\Omega$ the core-cladding interface ($\partial\Omega$ is a simple closed curve). Since Ω is translationally invariant, the transmission conditions (2.7-2.10) can be expressed as

$$E^{(1)} \times \hat{n} = E^{(2)} \times \hat{n} \quad \text{on } \partial\Omega, \quad (2.25)$$

$$H^{(1)} \times \hat{n} = H^{(2)} \times \hat{n} \quad \text{on } \partial\Omega, \quad (2.26)$$

$$n_1^2 E^{(1)} \cdot \hat{n} = n_2^2 E^{(2)} \cdot \hat{n} \quad \text{on } \partial\Omega, \quad (2.27)$$

$$H^{(1)} \cdot \hat{n} = H^{(2)} \cdot \hat{n} \quad \text{on } \partial\Omega. \quad (2.28)$$

where $\hat{n} = (n_x, n_y, 0)$. Then from (2.25-2.28) the z -components E_z and H_z are required to satisfy

$$E_z^{(1)} = E_z^{(2)} \quad \text{on } \partial\Omega,$$

$$H_z^{(1)} = H_z^{(2)} \quad \text{on } \partial\Omega.$$

These conditions are not enough to define well-posed problems for E_z and H_z . Additional boundary conditions can be extracted from Maxwell's equations and equations (2.7- 2.10) or (2.25-2.28). From the first equation in (2.6), we find

$$\begin{aligned} \nabla \times (\mathbb{E}^{(1)} - \mathbb{E}^{(2)}) \times \hat{n} &= i\omega\mu_0(\mathbb{H}^{(1)} - \mathbb{H}^{(2)}) \times \hat{n} \quad \text{on } \partial\Omega \\ &= 0, \end{aligned}$$

or

$$(\nabla \times \mathbb{E}^{(1)}) \times \hat{n} = (\nabla \times \mathbb{E}^{(2)}) \times \hat{n} \quad \text{on } \partial\Omega.$$

The z -component of this equation is

$$\begin{aligned} & -n_x \frac{\partial E_z^{(1)}}{\partial x} - n_y \frac{\partial E_z^{(1)}}{\partial y} + i\beta(-n_x E_x^{(1)} - n_y E_y^{(1)}) \\ &= -n_x \frac{\partial E_z^{(2)}}{\partial x} - n_y \frac{\partial E_z^{(2)}}{\partial y} + i\beta(-n_x E_x^{(2)} - n_y E_y^{(2)}) \quad \text{on } \partial\Omega. \end{aligned}$$

This implies that

$$\frac{\partial E_z^{(1)}}{\partial n} = \frac{\partial E_z^{(2)}}{\partial n} \quad \text{on } \partial\Omega.$$

Similarly, we obtain

$$\begin{aligned} \left[\frac{1}{n_1^2} \nabla \times \mathbb{H}^{(1)} - \frac{1}{n_2^2} \nabla \times \mathbb{H}^{(2)} \right] \times \hat{n} &= -i\omega\varepsilon_0(\mathbb{E}^{(1)} - \mathbb{E}^{(2)}) \times \hat{n} \\ &= 0 \quad \text{on } \partial\Omega. \end{aligned}$$

Hence, $\frac{1}{n_1^2} \nabla \mathbb{H}^{(1)} \times \hat{n} = \frac{1}{n_2^2} \nabla \mathbb{H}^{(2)} \times \hat{n} \quad \text{on } \partial\Omega$. The z -component of this equation yields

$$\frac{1}{n_1^2} \frac{\partial H_z^{(1)}}{\partial n} = \frac{1}{n_2^2} \frac{\partial H_z^{(2)}}{\partial n} \quad \text{on } \partial\Omega.$$

So, we have shown

Proposition 2.3.3 *The weakly-guiding approximation of Maxwell's equations yields the scalar Helmholtz or 2D wave equations for E_z and H_z*

$$\Delta E_z + (k^2 n^2 - \beta^2) E_z = 0 \quad \text{in } \mathbb{R}^2 \quad (2.29)$$

with E_z and $\frac{\partial E_z}{\partial n}$ continuous across $\partial\Omega$ and

$$\Delta H_z + (k^2 n^2 - \beta^2) H_z = 0 \quad \text{in } \mathbb{R}^2 \quad (2.30)$$

with H_z and $\frac{1}{n^2} \frac{\partial H_z}{\partial n}$ continuous across $\partial\Omega$.

Remark: The boundary conditions on E_z and H_z are slightly different. The normal derivative of E_z is required to be continuous across the media while that of H_z does not have to be.

CHAPTER 3

PERTURBATION OF GUIDED MODES IN CIRCULAR FIBERS

In the first half of the chapter, approximations of eigenvalues of a family of linear self-adjoint operators using the classical perturbation theory [20] are briefly considered. These approximation methods are later used to study the reduction of the signal bandwidth of weakly-guiding circular fibers whose refractive index profiles are slightly deviated from the optimal truncated parabolic shape.

3.1 Eigenvalue Approximations

In this section, we derive some useful approximations for eigenvalues of a self-adjoint operator based on the perturbation theory. Let H be a Hilbert space with the inner product (u, v) . Let L be a self-adjoint linear operator with domain of definition $D \subset H$. Let G be a domain of the complex ϵ -plane.

Definition 3.1.1 [20] *A family $L(\epsilon)$ of closed operator in a Hilbert space H is said to be analytic of type (A) over G if each domain of definition $D(L(\epsilon)) = D$ is independent of ϵ and $L(\epsilon)u$ is analytic for $\epsilon \in G$ for every $u \in D$.*

Definition 3.1.2 *A linear operator A is said to be relatively bounded with respect to L if $D(A) = D(L) = D$ and there exist nonnegative constants a and b such that*

$$\|Au\| \leq a\|u\| + b\|Lu\| \quad \forall u \in D. \quad (3.1)$$

Let $\lambda_0 \in \mathbb{R}$ be an isolated eigenvalue of L and u_0 be the corresponding normalized eigenvector, i.e.,

$$Lu_0 = \lambda_0 u_0.$$

If $|\epsilon|$ is sufficiently small, eigenvalues $\lambda(\epsilon)$ and corresponding normalized eigenvectors $u(\epsilon)$ of an analytic family of type (A), $\{L(\epsilon)\}$, are also analytic functions in ϵ , and moreover, $u(\epsilon)$ and $\lambda(\epsilon)$ have Taylor expansions

$$\begin{aligned} u(\epsilon) &= u_0 + \epsilon u^{(1)} + \epsilon^2 u^{(2)} + \dots, \\ \lambda(\epsilon) &= \lambda_0 + \epsilon \lambda^{(1)} + \epsilon^2 \lambda^{(2)} + \dots, \end{aligned}$$

with $L(0)u_0 = Lu_0$. Thus, the eigenvalue equations

$$L(\epsilon)u(\epsilon) = \lambda(\epsilon)u(\epsilon) \tag{3.2}$$

can be written as

$$L(\epsilon)(u_0 + \epsilon u^{(1)} + \dots) = \lambda(\epsilon)(u_0 + \epsilon u^{(1)} + \dots). \tag{3.3}$$

Hence, the first-order approximation of this equation is

$$L(\epsilon)u_0 = \lambda(\epsilon)u_0 + \mathcal{O}(\epsilon). \tag{3.4}$$

Thus, we obtain the first simple formula which is widely used [28]

$$\lambda(\epsilon) = \lambda_0 + ([L(\epsilon) - L]u_0, u_0). \tag{3.5}$$

In ([20], p.421), the eigenvalue problem is restricted to the finite system of eigenvalues - a finite collection of eigenvalues with finite multiplicities. Hence, the perturbation theory of the finite dimensional spaces (for matrices) can be applied without much modification. We will adapt this approach. Let λ be an isolated eigenvalue of the

unperturbed self-adjoint operator $L = L(0)$ with multiplicity m . Let P be the associated eigenprojection (here, the eigennilpotent D is identically zero because of the self-adjointness of L). The eigenvalue λ will in general split into several eigenvalues of $L(\epsilon)$ for small ϵ and form the so-called λ -group. Then the projection $P(\epsilon)$ for this λ -group is analytic in at $\epsilon = 0 \in G$. Let $M(\epsilon) := P(\epsilon)H$ be the invariant subspace under the perturbed operator $L(\epsilon)$. The λ -group eigenvalues of $L(\epsilon)$ are then the eigenvalues of $L(\epsilon)$ in the subspace $M(\epsilon)$. Thus, in order to determine the eigenvalues in the λ -group, we only need to solve the eigenvalue in the finite dimensional subspace $M(\epsilon)$.

Definition 3.1.3 *The weighted mean of the λ -group eigenvalues of $L(\epsilon)$ is defined as*

$$\begin{aligned}\hat{\lambda}(\epsilon) &:= \frac{1}{m} \text{tr}(L(\epsilon)P(\epsilon)) \\ &= \lambda + \frac{1}{m} \text{tr}((L(\epsilon) - \lambda)P(\epsilon)).\end{aligned}$$

If there is no splitting of λ so that the λ -group consists of only one eigenvalue $\lambda(\epsilon)$ with the same multiplicity m as λ , we have

$$\hat{\lambda}(\epsilon) \equiv \lambda(\epsilon).$$

Proposition 3.1.4 *Suppose that L has a finite number of isolated eigenvalues*

$\{\lambda, \mu_1, \mu_2, \dots, \mu_N\}$, where the eigenvalues μ_k are different from λ . Let $P = P(0)$ and $\{P_k\}$ be the corresponding eigenprojections. Then the weighted average eigenvalue $\hat{\lambda}(\epsilon)$ is of the form

$$\hat{\lambda}(\epsilon) = \lambda + \epsilon \hat{\lambda}^{(1)} + \epsilon^2 \hat{\lambda}^{(2)} + \dots$$

where

$$\hat{\lambda}^{(1)} = \frac{1}{m} \text{tr} L^{(1)} P(0), \tag{3.6}$$

$$\hat{\lambda}^{(2)} = \frac{1}{m} \text{tr}(L^{(2)}P(0) - L^{(1)}SL^{(1)}P(0)), \quad (3.7)$$

and

$$Su = \sum_{\mu_k \neq \lambda} \frac{P_k u}{\mu_k - \lambda}.$$

Proof: Let \mathcal{P} be the total eigenprojection for L , i.e.,

$$L\mathcal{P} = \sum_{\mu_i \in \{\lambda, \mu_k\}} \mu_i P_i.$$

For $|\epsilon|$ sufficiently small, we have

$$L(\epsilon)\mathcal{P}(\epsilon) = \sum_{\mu_i(\epsilon) \in \{\lambda(\epsilon), \mu_k(\epsilon)\}} \mu_i(\epsilon) P_i(\epsilon)$$

where

$$P_i(\epsilon) = P_i + \sum_{n=1}^{\infty} \epsilon^n P_i^{(n)}.$$

Then the proposition is proved using the standard perturbation theory in the finite dimensional case. ■

Assume that the eigenvalue λ_0 is simple ($m = 1$). Since the normalized eigenvectors of L form an orthonormal basis for the finite dimensional subspace $\mathcal{P}H$, we can express the formulas in the previous proposition as

$$\hat{\lambda}^{(1)} = (L^{(1)}u, u), \quad (3.8)$$

$$\hat{\lambda}^{(2)} = (L^{(2)}u, u) - \sum_{\mu_j \neq \lambda_0} \frac{(L^{(1)}u, v_j)(L^{(1)}v_j, u)}{\mu_j - \lambda_0}, \quad (3.9)$$

where u and v_j are the associated orthonormal eigenvectors of λ and μ_j , respectively.

In fact, the operator S is of the form

$$\begin{aligned} Sw &= \sum_{\mu_j \neq \lambda_0} (\mu_j - \lambda_0)^{-1} P_j w \\ &= \sum_{\mu_j \neq \lambda_0} (\mu_j - \lambda_0)^{-1} (w, v_j) v_j \quad \forall w \in H. \end{aligned}$$

The size of $|\epsilon|$ determines the accuracy of the approximations in (3.5,3.8,3.9). We will use these formulas to compute the perturbed eigenvalues later. We now derive an upper bound for $|\epsilon|$ such that the formulas in (3.5,3.8,3.9) are applicable. The technique used here is based on the theory of perturbation of a *relatively bounded operator*.

Definition 3.1.5 *Let L be a closed operator in H and ζ be a complex number. If $L - \zeta$ is invertible with*

$$R_\zeta(L) := (L - \zeta)^{-1} \quad (3.10)$$

then ζ is said to belong to the resolvent set of L . The operator-valued function $R_\zeta(L)$ defined on the resolvent set $P(L)$ is called the resolvent of L .

Let us consider a family of self-adjoint perturbed operators $L(\epsilon)$ of the form

$$L(\epsilon) = L + \epsilon L^{(1)}, \quad D(L(\epsilon)) = D(L) =: D, \quad (3.11)$$

where $L^{(1)}$ is a relatively bounded operator with respect to L ,

$$\|L^{(1)}u\| \leq a\|u\| + b\|Lu\|, \quad u \in D, \quad (3.12)$$

where a and b are nonnegative constants. Let ζ be a point in the resolvent set $P(L)$ of L . Since L is self-adjoint, we have ([20], p.272)

$$\begin{aligned} \|R_\zeta(L)\| &= \|(L - \zeta)^{-1}\| \\ &= \operatorname{spr} R_\zeta(L) \\ &= \sup_{\lambda \in \sigma(L)} \frac{1}{|\zeta - \lambda|} \\ &= \frac{1}{\operatorname{dist}(\zeta, \sigma(L))} \end{aligned}$$

$$= \frac{1}{d},$$

where $\sigma(L)$ is the spectrum of L . The next lemma gives a necessary upper bound for $|\epsilon|$ so that a point ζ in the resolvent set of L is also an element in the resolvent set of the perturbed operator $L(\epsilon)$.

Lemma 3.1.6 *Let $L(\epsilon) = L + \epsilon L^{(1)}$ be self-adjoint in H and $L^{(1)}$ satisfy (3.12). Let ζ be a point in the resolvent set of L . If*

$$|\epsilon| < \frac{d}{a + b(|\zeta| + d)} =: \frac{1}{\delta(\zeta)}, \quad (3.13)$$

then ζ is also in the resolvent set of $L(\epsilon)$. Moreover,

$$R_\zeta(L_\epsilon) := (L(\epsilon) - \zeta)^{-1} = \sum_{n=1}^{\infty} B_n \epsilon^n, \quad (3.14)$$

where

$$B_0 = R_\zeta(L), \quad (3.15)$$

$$B_n = (-1)^n R_\zeta(L) [L^{(1)} R_\zeta(L)]^n, \quad (3.16)$$

and

$$\|B_n\| \leq \frac{\delta(\zeta)^n}{d}, \quad n = 1, 2, 3, \dots \quad (3.17)$$

Proof: Let $\zeta \in P(L)$ - the resolvent set of L . In order for $\zeta \in P(L(\epsilon))$, $L(\epsilon) - \zeta$ must be invertible, i.e., $(L(\epsilon) - \zeta)^{-1}$ exists and bounded. We write

$$\begin{aligned} L(\epsilon) - \zeta &= \epsilon L^{(1)} + L - \zeta \\ &= [I + \epsilon L^{(1)} R_\zeta(L)](L - \zeta). \end{aligned}$$

Since $\zeta \in P(L)$, $R_\zeta(L) = (L - \zeta)^{-1}$ is well-defined. Hence we only need to show that $I + \epsilon L^{(1)} R_\zeta(L)$ is invertible for some ϵ . The Neumann series of $[I + \epsilon L^{(1)} R_\zeta(L)]^{-1}$ converges absolutely if

$$|\epsilon| \|L^{(1)} R_\zeta(L)\| < 1.$$

Since $L^{(1)}$ is L -bounded, for $u \in H$, we have

$$\begin{aligned}
\|L^{(1)}R_\zeta(L)u\| &\leq a\|R_\zeta(L)u\| + b\|LR_\zeta(L)u\| \\
&\leq (a\|R_\zeta(L)\| + b\|LR_\zeta(L)\|) \|u\| \\
&\leq \left[a\frac{1}{d} + b\left(\frac{|\zeta|}{d} + 1\right) \right] \|u\|.
\end{aligned}$$

The last inequality can be seen from noticing

$$(L - \zeta)R_\zeta(L) = I,$$

so,

$$LR_\zeta(L) = \zeta R_\zeta(L) + I, \quad (3.18)$$

and, hence

$$\begin{aligned}
\|LR_\zeta(L)\| &\leq |\zeta|\|R_\zeta(L)\| + \|I\| \\
&\leq \frac{|\zeta|}{d} + 1.
\end{aligned}$$

Therefore,

$$\|L^{(1)}R_\zeta(L)\| \leq \frac{1}{d}[a + b(|\zeta| + d)] =: \delta(\zeta). \quad (3.19)$$

Thus, if $|\epsilon| < \frac{1}{\delta(\zeta)}$, the operator $I + \epsilon L^{(1)}R_\zeta(L)$ is invertible. It implies that $L(\epsilon) - \zeta$ is invertible and therefore ζ is also a point in the resolvent set of $L(\epsilon)$. We now can express $(L(\epsilon) - \zeta)^{-1}$ as a Neumann series:

$$R_\zeta(L(\epsilon)) = R_\zeta(L) \sum_{n=0}^{\infty} [L^{(1)}R_\zeta(L)]^n \epsilon^n \quad (3.20)$$

$$= R_\zeta(L) + \sum_{n=1}^{\infty} R_\zeta(L)[L^{(1)}R_\zeta(L)]^n \epsilon^n. \quad (3.21)$$

Let us denote

$$B_0 = R_\zeta(L),$$

and

$$B_n = R_\zeta(L)[L^{(1)}R_\zeta(L)]^n, \quad n = 1, 2, \dots$$

Finally, for $n = 1, 2, \dots$,

$$\begin{aligned} \|B_n\| &\leq \|R_\zeta(L)\| \|L^{(1)}R_\zeta(L)\|^n \\ &\leq \frac{1}{d} \delta(\zeta)^n. \end{aligned}$$

This completes the proof. ■

Definition 3.1.7 Let $\lambda_0 \in \sigma(L)$ be an isolated eigenvalue. Let $\Lambda = \sigma(L) - \lambda_0$. The isolation distance of λ_0 is defined as

$$d = \text{dist}(\lambda_0, \Lambda). \quad (3.22)$$

Let λ_0 be an isolated eigenvalue of multiplicity $m < \infty$ with isolation distance d and u_0 the corresponding normalized eigenvector. Let Γ be the circle center λ_0 and radius $\frac{d}{2}$. We set

$$\delta := \max_{\zeta \in \Gamma} \delta(\zeta) \quad (3.23)$$

where $\delta(\zeta)$ is defined in (3.19). With these assumptions, we state the next theorem which can be used to estimate the coefficients of the Taylor expansions of the eigenvalues $\lambda(\epsilon)$ and corresponding normalized eigenvectors $u(\epsilon)$.

Theorem 3.1.8 Let δ be as in (3.23). If $|\epsilon| < \frac{1}{2\delta}$, the circle Γ (center λ_0 , radius $d/2$) encloses exactly m (repeated) real eigenvalues $\lambda(\epsilon)$ of $L(\epsilon)$ and no other points of $\sigma(L(\epsilon))$. Moreover, if λ_0 is a simple isolated eigenvalue ($m = 1$), then

$$\lambda(\epsilon) = \lambda_0 + \epsilon \lambda^{(1)} + \epsilon^2 \lambda^{(2)} + \dots, \quad (3.24)$$

$$u(\epsilon) = u_0 + \epsilon u^{(1)} + \epsilon^2 u^{(2)} + \dots, \quad (3.25)$$

where

$$|\lambda^{(n)}| \leq \frac{d}{2} \delta^n, \quad n = 1, 2, \dots, \quad (3.26)$$

$$\|u^{(n)}\| \leq 2^n \delta^n, \quad n = 1, 2, \dots \quad (3.27)$$

Proof: Since $|\epsilon| < \frac{1}{2\delta} < \frac{1}{\delta}$, any point on the circle Γ is in the resolvent set of $L(\epsilon)$ by the previous lemma. Then from (3.14),

$$R_\zeta(L(\epsilon)) = \sum_{n=0}^{\infty} B_n \epsilon^n, \quad B_0 = R_\zeta(L),$$

converges uniformly on the compact set Γ . Hence, the eigenprojection $E(\epsilon)$ can be expressed as

$$\begin{aligned} E(\epsilon) &:= -\frac{1}{2\pi i} \oint_{\Gamma} R_\zeta(L(\epsilon)) d\zeta \\ &= -\frac{1}{2\pi i} \sum_{n=0}^{\infty} \epsilon^n \oint_{\Gamma} B_n d\zeta \\ &= -\frac{1}{2\pi i} \oint_{\Gamma} R_\zeta(L) d\zeta + \sum_{n=1}^{\infty} \epsilon^n \left(-\frac{1}{2\pi i} \oint_{\Gamma} B_n d\zeta \right) \\ &= E_0 + \sum_{n=1}^{\infty} E_n \epsilon^n, \end{aligned}$$

where

$$\|E_n\| \leq \frac{1}{2\pi} \oint_{\Gamma} \|B_n\| |d\zeta| \leq \frac{\delta^n}{2}, \quad n = 1, 2, \dots \quad (3.28)$$

Thus,

$$\begin{aligned} \|E(\epsilon) - E_0\| &\leq \sum_{n=1}^{\infty} |\epsilon|^n \|E_n\| \leq \frac{1}{2} \sum_{n=1}^{\infty} \delta^n \epsilon^n \\ &= \frac{1}{2} \left(\frac{1}{1 - \delta\epsilon} - 1 \right) = \frac{1}{2} \frac{\epsilon\delta}{1 - \epsilon\delta} < \frac{1}{2}. \end{aligned}$$

Since $E(\epsilon)$ and E_0 are eigenprojections with $\|E(\epsilon) - E_0\| < 1$, $E(\epsilon)(H)$ and $E_0(H)$ are isomorphic, i.e., $\dim E(\epsilon)(H) = \dim E_0(H)$. Thus, the eigenspace corresponding to the part of the spectrum of $L(\epsilon)$ in the interior of Γ has the same dimension as the eigenspace of λ_0 . Hence, if λ_0 is a simple isolated eigenvalue ($m = 1$), there exists exactly one $\lambda(\epsilon)$ inside Γ which is an eigenvalue of $L(\epsilon)$. This fact is important in numerical computation.

Let

$$u(\epsilon) := \frac{E(\epsilon)u_0}{\|E(\epsilon)u_0\|}. \quad (3.29)$$

Since $E(\epsilon)$ is an eigenprojection,

$$L(\epsilon)u(\epsilon) = \lambda(\epsilon)u(\epsilon).$$

Then,

$$u(\epsilon) = \frac{\left(E_0 + \sum_{n=1}^{\infty} \epsilon^n E_n\right) u_0}{\left(\left(E_0 + \sum_{n=1}^{\infty} \epsilon^n E_n\right) u_0, u_0\right)^{1/2}}.$$

Since $(E_0 u_0, u_0) = (u_0, u_0) = 1$, we get

$$u(\epsilon) = \frac{E_0 u_0 + \sum_{n=1}^{\infty} \epsilon^n E_n u_0}{\left[1 + \sum_{n=1}^{\infty} \epsilon^n (E_n u_0, u_0)\right]^{1/2}}. \quad (3.30)$$

The series (3.30) converges for $|\epsilon| < \frac{1}{2\delta}$. In fact, using binomial expansion and $\|E_n\| \leq \delta^2$, we see that

$$\begin{aligned} & \left(1 + \sum_{n=1}^{\infty} |\epsilon|^n \delta^n\right) \left[\sum_{m=0}^{\infty} \left|\binom{-\frac{1}{2}}{m}\right| \left(\sum_{n=1}^{\infty} |\epsilon|^n \delta^n\right)^m\right] \\ &= \frac{1}{1 - \epsilon\delta} \cdot \sum_{m=0}^{\infty} \left|\binom{-\frac{1}{2}}{m}\right| \cdot \left(\frac{\epsilon\delta}{1 - \epsilon\delta}\right)^m \end{aligned}$$

$$\begin{aligned}
&= \frac{1}{1 - \epsilon\delta} \cdot \frac{1}{\left(1 - \frac{\epsilon\delta}{1 - \epsilon\delta}\right)^{1/2}} \\
&= (1 - \epsilon\delta)^{-1/2} \cdot (1 - 2\epsilon\delta)^{-1/2} \leq (1 - 2\epsilon\delta)^{-1}.
\end{aligned}$$

which is strictly less than 1 provided that $|\epsilon| < \frac{1}{2\delta}$. Thus, we write

$$u(\epsilon) = u_0 + \sum_{n=1}^{\infty} u_n \epsilon^n$$

where

$$\|u_n\| \leq 2^n \delta^n. \quad (3.31)$$

This shows the approximation for the eigenvector $u(\epsilon)$. Now, we derive an approximation for $\lambda(\epsilon)$. Again, since $L(\epsilon)u(\epsilon) = \lambda(\epsilon)u(\epsilon)$, $(L(\epsilon) - \lambda_0)u(\epsilon) = (\lambda(\epsilon) - \lambda_0)u(\epsilon)$. So,

$$\begin{aligned}
\lambda(\epsilon) - \lambda_0 &= \frac{((L(\epsilon) - \lambda_0)u(\epsilon), u_0)}{(u(\epsilon), u_0)} \\
&= \frac{((L(\epsilon) - \lambda_0)E(\epsilon)u_0, u_0)}{(E(\epsilon)u_0, u_0)}. \quad (3.32)
\end{aligned}$$

Since $L(\epsilon)$ is closed and $R_\zeta(L)$ is continuous (bounded) in ζ and $\text{Ran}(R_\zeta(L(\epsilon))) \subset D(L(\epsilon))$, we have

$$\begin{aligned}
(L(\epsilon) - \lambda_0)E(\epsilon) &= (L(\epsilon) - \lambda_0) \left(-\frac{1}{2\pi i} \oint_{\Gamma} R_\zeta(L(\epsilon)) d\zeta \right) \\
&= -\frac{1}{2\pi i} \oint_{\Gamma} (L(\epsilon) - \lambda_0) R_\zeta(L(\epsilon)) d\zeta \\
&= -\frac{1}{2\pi i} \oint_{\Gamma} L(\epsilon) R_\zeta(L(\epsilon)) d\zeta - \lambda_0 \left(-\frac{1}{2\pi i} \oint_{\Gamma} R_\zeta(L(\epsilon)) d\zeta \right) \\
&= -\frac{1}{2\pi i} \oint_{\Gamma} [I + \zeta R_\zeta(L(\epsilon))] d\zeta
\end{aligned}$$

$$\begin{aligned}
& -\lambda_0 \left(-\frac{1}{2\pi i} \oint_{\Gamma} R_{\zeta}(L(\epsilon)) d\zeta \right) \\
&= -\frac{1}{2\pi i} \oint_{\Gamma} (\zeta - \lambda_0) R_{\zeta}(L(\epsilon)) d\zeta \\
&= \sum_{n=0}^{\infty} \epsilon^n \left[-\frac{1}{2\pi i} \oint_{\Gamma} (\zeta - \lambda_0) B_n d\zeta \right] \\
&=: \sum_{n=0}^{\infty} \epsilon^n C_n.
\end{aligned}$$

Since $B_0 = R_{\zeta}(L)$, $C_0 = 0$. In fact,

$$\begin{aligned}
-\frac{1}{2\pi i} \oint_{\Gamma} (\zeta - \lambda_0) B_0 d\zeta &= -\frac{1}{2\pi i} \oint_{\Gamma} (\zeta - \lambda_0) R_{\zeta}(L) d\zeta \\
&= -\frac{1}{2\pi i} \oint_{\Gamma} (\zeta - \lambda_0)(L - \zeta)^{-1} d\zeta \\
&= -\frac{1}{2\pi i} \oint_{\Gamma} \zeta (L - \zeta)^{-1} d\zeta - \lambda_0 \left(-\frac{1}{2\pi i} \oint_{\Gamma} (L - \zeta)^{-1} d\zeta \right) \\
&= -\frac{1}{2\pi i} \oint_{\Gamma} [I + L R_{\zeta}(L)] d\zeta - \lambda_0 \left(-\frac{1}{2\pi i} \oint_{\Gamma} (L - \zeta)^{-1} d\zeta \right) \\
&= L \left(-\frac{1}{2\pi i} \oint_{\Gamma} R_{\zeta}(L) d\zeta \right) - \lambda_0 \left(-\frac{1}{2\pi i} \oint_{\Gamma} R_{\zeta}(L) d\zeta \right) \\
&= L E_0 - \lambda_0 E_0 \\
&\equiv 0.
\end{aligned}$$

For $n = 1, 2, 3, \dots$,

$$\|C_n\| \leq \frac{1}{2\pi} \oint_{\Gamma} |\zeta - \lambda_0| \|B_n\| |d\zeta|$$

$$\leq \frac{d}{2} \cdot d \cdot \frac{\delta^n}{d} = \frac{d}{2} \delta^n. \quad (3.33)$$

Finally, from (3.32), we obtain

$$\begin{aligned} \lambda(\epsilon) - \lambda_0 &= \frac{\sum_{n=1}^{\infty} \epsilon^n (C_n u_0, u_0)}{\left[1 + \sum_{n=1}^{\infty} \epsilon^n (E_n u_0, u_0) \right]} \\ &= \sum_{n=1}^{\infty} \epsilon^n (C_n u_0, u_0) \cdot \sum_{m=0}^{\infty} (-1)^m \left[\sum_{n=1}^{\infty} \epsilon^n (E_n u_0, u_0) \right]^m. \end{aligned}$$

Since $\|C_n\| \leq \frac{d}{2} \delta^n$, $\|E_n\| \leq \frac{\delta^n}{2}$, the right hand side of the previous equation is bounded by

$$\begin{aligned} \frac{d}{2} \sum_{n=1}^{\infty} \epsilon^n \delta^n \cdot \sum_{m=0}^{\infty} \left(\sum_{n=1}^{\infty} \epsilon^n \frac{\delta^n}{2} \right)^m &= \frac{d}{2} \sum_{n=1}^{\infty} \epsilon^n \delta^n \cdot \frac{1}{1 - \frac{\epsilon \delta}{2(1-\epsilon \delta)}} \\ &= \frac{d}{2} \cdot \frac{2(1-\epsilon \delta)}{2(1-\frac{3}{2}\epsilon \delta)} \cdot \sum_{n=1}^{\infty} \epsilon^n \delta^n \\ &< \frac{d}{2} \sum_{n=0}^{\infty} \epsilon^n \delta^n. \end{aligned} \quad (3.34)$$

Hence, from (3.33) and (3.34), we have

$$\lambda(\epsilon) = \lambda_0 + \sum_{n=1}^{\infty} \lambda_n \epsilon^n,$$

where $|\lambda_n| < \frac{d}{2} \delta^n$. This completes the proof. ■

In Section 7, these approximations are applied to compute the perturbed propagation constants of circular fibers.

3.2 Scalar Wave Equation E_z

In Chapter 2, we derived the Helmholtz equation and the boundary conditions (2.29) for the longitudinal component $E_z e^{-i\beta z}$ of the time-harmonic electric field \mathbb{E} .

The circular symmetry of a fiber allows us to reduce the Helmholtz equation to an ordinary differential equation using polar coordinates. Let (r, θ) be the polar coordinates in \mathbb{R}^2 . Assume that the index profile n is radially symmetric and z -invariant, i.e., $n = n(r)$. Then the Helmholtz equation for E_z becomes

$$\frac{\partial^2 E_z}{\partial r^2} + \frac{1}{r} \frac{\partial E_z}{\partial r} + \frac{1}{r^2} \frac{\partial^2 E_z}{\partial \theta^2} + (k^2 n^2 - \beta^2) E_z = 0. \quad (3.35)$$

Using separation of variables, we write

$$E_z = \Psi(r) \Phi(\theta) e^{-i\beta z}.$$

Then $\Psi(r)$ and $\Phi(\theta)$ satisfy the equations

$$\frac{d^2 \Phi}{d\theta^2} + m^2 \Phi = 0, \quad (3.36)$$

$$\frac{d^2 \Psi}{dr^2} + \frac{1}{r} \frac{d\Psi}{dr} + \left(k^2 n^2 - \beta^2 - \frac{m^2}{r^2} \right) \Psi = 0, \quad (3.37)$$

where m must be an integer, since it is required that the field is self-consistent on each rotation of θ through 2π . Thus,

$$\Phi(\theta) = \begin{cases} \cos(\alpha + m\theta), \\ \sin(\alpha + m\theta), \end{cases}$$

where α is a constant. The differential equation (3.37) for the function $\Psi(r)$ is called *Sturm-Liouville* equation. The boundary conditions for Ψ are

$$\lim_{r \rightarrow 0} \sqrt{r} \Psi(r) = 0,$$

$$\lim_{r \rightarrow \infty} \sqrt{r} \Psi(r) = 0.$$

We also assume that $\Psi(r)$ and $\Psi'(r)$ are continuous in $(0, \infty)$ by the transmission conditions. For each m , the propagation constants β of guided modes have to satisfy the double inequalities [32]

$$kn_{cl} < \beta \leq kn_{co}. \quad (3.38)$$

This gives us the range of allowed eigenvalues. The performance of a fiber depends on the group time delays for the propagating modes.

Definition 3.2.1 *The time delay per unit length of each propagating mode is*

$$\tau = \frac{1}{c} \frac{d\beta}{dk} \quad (3.39)$$

where c is the speed of light in free space, and $k = 2\pi/\lambda$.

The time delay τ can also be defined as follows. For convenience, (3.37) is rewritten as

$$-\frac{1}{r}(r\Psi')' + \left\{ \frac{m^2}{r^2} - k^2 n^2(r) + \beta^2 \right\} \Psi = 0. \quad (3.40)$$

Let (β_1, Ψ_1) and (β_2, Ψ_2) be solutions of (3.40) for $k = k_1$ and $k = k_2$, respectively.

Then, by integration by parts, we have

$$(\beta_2^2 - \beta_1^2) \int_0^\infty \Psi_1 \Psi_2 r dr = (k_2^2 - k_1^2) \int_0^\infty n^2 \Psi_1 \Psi_2 r dr.$$

So, if $\beta_1 = \beta(k)$, $\beta_2 = \beta(k+h)$, and $h \rightarrow 0$ and since the eigenfunctions $\Psi(r, k)$ smoothly depend on k , (Chap.1, Theorem 8.4 in [7]), we have

$$2\beta \frac{d\beta}{dk} \int_0^\infty \Psi^2 r dr = 2k \int_0^\infty n^2(r) \Psi^2 r dr.$$

Hence, the time delay is

$$\tau = \frac{1}{c} \frac{k}{\beta} \frac{\int_0^\infty n^2(r) \Psi^2(r) r dr}{\int_0^\infty \Psi^2(r) r dr}. \quad (3.41)$$

With this integral formula, we can avoid the numerical differentiation in calculating τ .

3.3 Perturbed Fibers

In this section, a "perturbed" index profile is the result of adding a small perturbation to the "unperturbed" profile whose solutions of the scalar wave equation

are known. If the deviation from the known profile is small enough, perturbation methods provide a good approximation to the solutions of the perturbed (unknown) fiber. Define the perturbed index profile

$$\tilde{n}(r) = \begin{cases} n(r) + \epsilon b(r) & 0 \leq r \leq a, \\ n_{cl} & r > a \end{cases}$$

where $b(r)$ is a bounded function and ϵ is between 1% and 10% of the difference $(n_{co} - n_{cl})$. The perturbed eigenvalues associated to the perturbed index profiles can be approximated by the formulas (3.5), (3.9), and (3.26) where L is the Sturm-Liouville operator defined by

$$L := -\frac{1}{r} \frac{d}{dr} \left(r \frac{d}{dr} \right) + \left\{ \frac{m^2}{r^2} - k^2 n^2(r) \right\} \quad (3.42)$$

and the perturbed operator is

$$L(\epsilon) := L - \epsilon 2n(r)b(r) - \epsilon^2 b^2(r). \quad (3.43)$$

Hence, $L^{(1)} := 2n(r)b(r)$ and $L^{(2)} := b^2(r)$.

3.4 Truncated Parabolic Profile

The truncated parabolic profile is given as

$$n^2(R) = \begin{cases} n_{co}^2(1 - 2\Delta R^2) & 0 \leq R \leq 1, \\ n_{cl}^2 & R > 1, \end{cases}$$

where $R = r/a$ and a is the core radius. The scalar wave equation is normalized to

$$\left\{ \frac{d^2}{dR^2} + \frac{1}{R} \frac{d}{dR} - \frac{m^2}{R^2} + a^2 [k^2 n^2(R) - \beta^2] \right\} \Psi(R) = 0, \quad R \in (0, \infty).$$

Let's define the following parameters [32]:

$$V = ak\sqrt{n_{co}^2 - n_{cl}^2}, \quad (3.44)$$

$$U = a\sqrt{k^2 n_{co}^2 - \beta^2}, \quad (3.45)$$

$$W = a\sqrt{\beta^2 - k^2 n_{cl}^2}. \quad (3.46)$$

Substituting these parameters in the above equation, we get

$$\left\{ \frac{d^2}{dR^2} + \frac{1}{R} \frac{d}{dR} - \frac{m^2}{R^2} + U^2 - V^2 R^2 \right\} \Psi(R) = 0 \quad 0 \leq R \leq 1, \quad (3.47)$$

$$\left\{ \frac{d^2}{dR^2} + \frac{1}{R} \frac{d}{dR} - \frac{m^2}{R^2} - W^2 \right\} \Psi(R) = 0 \quad R > 1. \quad (3.48)$$

For each allowed m , the (exact) solutions, normalized at $R = 1$, are [34]

$$\Psi_{l,m}(R) = \begin{cases} \frac{M_{\kappa,\mu}(VR^2)}{RM_{\kappa,\mu}(V)} & 0 \leq R \leq 1, \\ \frac{K_m(WR)}{K_m(W)} & R > 1, \end{cases} \quad (3.49)$$

where $\kappa = \frac{U^2}{4V}$, $\mu = \frac{m}{2}$, and l the radial index. $M_{\kappa,\mu}(z)$ is the Whittaker function of the first kind [1]. It is an entire function in z and κ . $K_m(z)$ is the modified Bessel function of the second kind [1]. To find the propagation constants $\beta_{l,m}$, we utilize the continuity conditions on $\Psi(R)$ and $\Psi'(R)$ and get the eigenvalue equation

$$2V \frac{M'_{\kappa,\mu}(V)}{M_{\kappa,\mu}(V)} - 1 = W \frac{K'_m(W)}{K_m(W)}. \quad (3.50)$$

Remarks: The Whittaker function of the first kind is defined as

$$\begin{aligned} M_{\kappa,\mu}(z) &= e^{-\frac{z}{2}} z^{\frac{1}{2}+\mu} {}_1F_1\left(\frac{1}{2} + \mu - \kappa, 2\mu + 1, z\right) \\ &= e^{-\frac{z}{2}} z^{\frac{1}{2}+\mu} \sum_{n=0}^{\infty} \frac{\left(\frac{1}{2} + \mu - \kappa\right)_n}{(2\mu + 1)_n} \frac{z^n}{n!} \end{aligned}$$

where $(p)_n = p(p+1)(p+2)\dots(p+n-1)$. This power series converges for all finite values of z and κ [33]. Hence, this function can be easily computed from this definition.

If the time delay τ is computed using the integral formula (3.41), it is convenient to use the integral identities of $K_m^2(WR)$ [32]

$$\begin{aligned} \int_1^{\infty} K_0^2(WR) R dR &= \frac{1}{2}(K_1^2(W) - K_0^2(W)), \\ \int_1^{\infty} K_m^2(WR) R dR &= \frac{1}{2}(K_{m-1}(W)K_{m+1}(W) - K_m^2(W)). \end{aligned}$$

3.5 Distortions

In this section, we consider several different types of distortions of the truncated parabolic profile. All of the following distortions are simulated by adding a perturbation function $p(R)$ to the truncated-parabolic profile $n(R)$.

(i) The ripple distortions (without the exponential term) is simulated by

$$p(R) = \epsilon \sin(2\pi NR). \quad (3.51)$$

The parameters are the amplitude ϵ which is between 1% and 15% of the difference $n_{co} - n_{cl}$ and the number of ripples which ranges from 1 to 20.

(ii) The ripple distortions with the exponential term decay exponentially away from the fiber axis and are simulated by

$$p(R) = \epsilon \sin(2\pi NR) \exp(-4R^2). \quad (3.52)$$

(iii) The dip distortion often occurs when fibers are made by the MCVD process. This distortion can be simulated by

$$p(R) = \begin{cases} n_{co}(1 - 2\Delta R^2)^{\frac{1}{2}} - b \cdot \exp\left(-\frac{R_0^2}{(R_0 - R)^2} + 1\right) & 0 \leq R \leq R_0, \\ 0 & \text{elsewhere} \end{cases} \quad (3.53)$$

where b is between 5% and 10% of $n_{co} - n_{cl}$ and R_0 is between 5% and 10% of the core radius.

(iv) The bulge distortions:

$$p(R) = \begin{cases} 0.001 \sin\{5\pi(R - R_0)\} & R_0 \leq R \leq R_0 + 0.2, \\ 0 & \text{elsewhere} \end{cases} \quad (3.54)$$

where the parameter R_0 is the location of the bulge.

3.6 Frequency Response and Bandwidth

There are at most finite number of propagating modes in a fiber. Each mode travels with different speed, hence arrives at the end of a 1km -long fiber at a different time. In [24] and [25], the impulse response is approximated as follows. The interval of the arrival times of all propagating modes (time spread) is divided into n time slots, for some suitable n , the number of guided modes arriving in each time slot is counted. The result is a step-function approximating the impulse response. The frequency response of a fiber is defined as the absolute modulus of the Fourier transform of the impulse response step-function. Then, the signal bandwidth is the half-maximum frequency of the frequency response. However, if the time spread is very large, this approximation of the impulse response yields inaccurate bandwidth. An alternative approach is given in [9]. Each mode is treated as an independent delta function. Thus, the pulse at 1km is the distribution of delta functions (spikes) with appropriately weighted amplitudes. More precisely, if τ_i , $i = 1, 2, \dots, N$, is the arrival time of each propagating mode and w_i is the corresponding modal weight, the pulse T is described by

$$T(t) = \sum_{i=1}^N w_i \delta(t - \tau_i) \quad (3.55)$$

where

$$\delta(t) = \begin{cases} 1 & t = 0, \\ 0 & t \neq 0. \end{cases}$$

The frequency response $F(\omega)$ is the absolute value of the Fourier transform of the pulse T ,

$$\begin{aligned} F(\omega) &= \left| \int_{-\infty}^{\infty} T(t) e^{-2\pi i t \omega} dt \right| \\ &= \frac{1}{2\pi} \left| \sum_{i=1}^N w_i e^{2\pi i \tau_i \omega} \right|. \end{aligned} \quad (3.56)$$

The fiber bandwidth is defined the same.

The truncated-parabolic fiber used here is described by

$$a = 31.25\mu m,$$

$$\lambda = 0.85\mu m,$$

$$n_{co} = 1.48\mu m,$$

$$n_{cl} = 1.46\mu m.$$

This particular fiber supports 210 guided modes, whose signal bandwidth is $1413MHz \cdot km$. All of the slightly perturbed fibers considered here also support the same number of guided modes but their signal bandwidths are reduced very significantly. This can be seen in the numerical experiments in the next section.

3.7 Numerical Experiments

3.7.1 First Order and Second Order Approximations

We first compare the eigenvalues found by the first and second order using (3.5) and (3.9) with those found by the finite element method (discussed in the next chapter). Here we use the ripple distortion without the exponential term with $\epsilon = 1\% \cdot (n_{co} - n_{cl}) = 2 \cdot 10^{-4}$ and 1 ripple and the operator $L(\epsilon) = L + \epsilon L^{(1)} + \epsilon^2 L^{(2)}$ defined in (3.43). For the finite element error in eigenvalues to be less than 10^{-10} , it requires 1024 mesh points for the fundamental mode ($m = 0, l = 0$) and 8192 mesh points for the higher mode ($m = 0, l = 6$), while the formulas (3.5) and (3.9) are easily computed. Therefore, the perturbation methods are much faster and less expensive especially for smaller propagation constants (*i.e.*, closer to the cut-off).

For the application of (3.26), we rewrite the operator $L^{(1)}$ as $L^{(1)} = 2n(r)b(r) + cb^2(r)$. For $m = 0$, the isolation distance of the largest exact eigenvalue of L , $\lambda_0 = 10.9348901$, is $d = 0.03$. We have $\|L^{(1)}\| \leq a\|u\| + b\|L\|$ where $a = 2n_{co} + \epsilon$, since

Table 3.1: Eigenvalues by First and Second Order and FEM for Ripple Distortion

Unperturbed	First order	Second order	FEM
10.9348901	10.9358125	10.9358229	10.9358230
10.8717622	10.8717934	10.8718034	10.8718035

$|b(r)| \leq 1$ and $b = 0$. So,

$$\delta = \frac{a}{d} = \frac{2 \cdot 1.48 + .0002}{d} = 296.02.$$

Therefore, the perturbed eigenvalue $\lambda(\epsilon)$ corresponding to λ_0 can be approximated by the Taylor series

$$\lambda(\epsilon) = \lambda_0 + \epsilon \lambda^{(1)} + \epsilon^2 \lambda^{(2)} + \dots$$

with $\epsilon = 2 \cdot 10^{-4}$ and $|\lambda^{(n)}| \leq \frac{d}{2} \delta^n = 5 \cdot 10^{-3} \times 296^n$. Hence,

$$|\lambda(\epsilon) - \lambda_0| \leq 9 \cdot 10^{-4} + \mathcal{O}(\epsilon^2).$$

This bound agrees with the result in the above table.

3.7.2 Bandwidths of Perturbed Fibers

Using the perturbation method, we compute the perturbed eigenvalues. Thus, the bandwidths of perturbed fibers can be approximated. We assume that all modes carry the same modal weight

$$w_i = \frac{1}{N}$$

where N is the total number of propagating modes. As we can see from the tables, fibers suffer a serious reduction in bandwidths when their index profiles are slightly deviated from the optimal shape. For example, in the table for ripple distortions without the exponential term, the bandwidth of the truncated parabolic fiber is dropped from $1413 \text{ MHz} \cdot \text{km}$ to $449 \text{ MHz} \cdot \text{km}$ when its profile is distorted with only

one ripple of amplitude $\epsilon = 1\% \cdot (n_{co} - n_{cl}) = .0002$. We plot the index profiles of different perturbed fibers and the associated impulse responses.

Table 3.2: Bandwidths of Ripple Distortions without exponential term: $p(R) = \epsilon \sin(2\pi NR)$.

ϵ	N	$BD(MHz \cdot km)$
$1\% \cdot (n_{co} - n_{cl})$	1	449
$1\% \cdot (n_{co} - n_{cl})$	5	174
$1\% \cdot (n_{co} - n_{cl})$	10	194
$1\% \cdot (n_{co} - n_{cl})$	15	1119
$1\% \cdot (n_{co} - n_{cl})$	20	1437 (noise)

Table 3.3: Bandwidths of Ripple Distortions with exponential term: $p(R) = \epsilon \sin(2\pi NR) \exp(-\frac{4}{R^2})$.

ϵ	N	$BD(MHz \cdot km)$
$1\% \cdot (n_{co} - n_{cl})$	10	557
$2\% \cdot (n_{co} - n_{cl})$	10	298
$5\% \cdot (n_{co} - n_{cl})$	10	121
$10\% \cdot (n_{co} - n_{cl})$	10	62

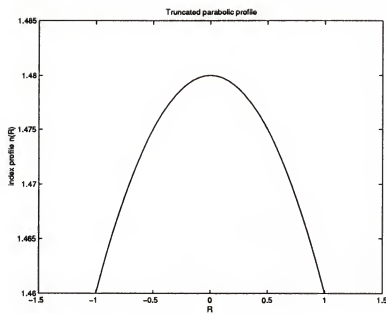


Figure 3.1: Truncated parabolic profile.

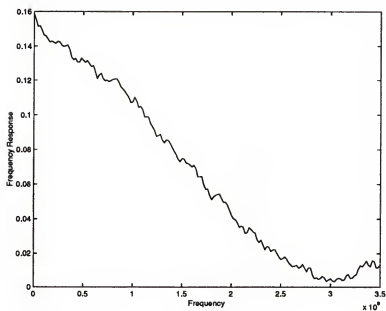


Figure 3.2: Frequency response of the truncated parabolic profile.

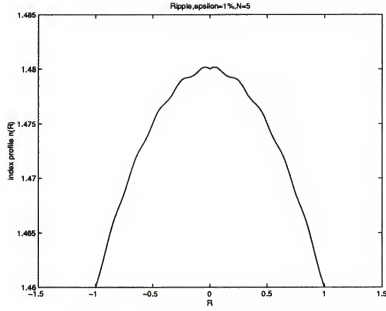


Figure 3.3: Ripple distortion profile, $N = 5$, $\epsilon = 1\% \cdot (n_{co} - n_{cl})$.

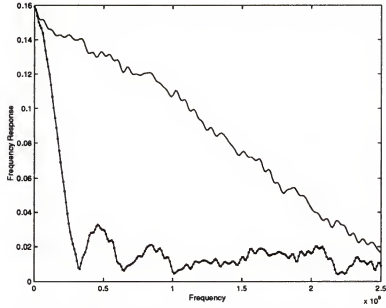


Figure 3.4: Frequency responses of the optimal profile (solid) and of the ripple distortion (dotted) with $N = 5$, $\epsilon = 1\% \cdot (n_{co} - n_{cl})$.

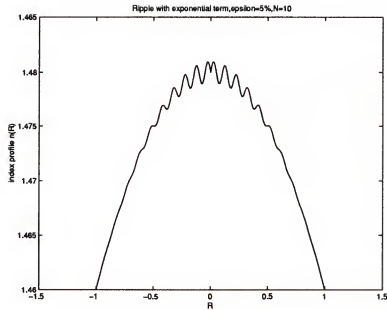


Figure 3.5: Ripple distortion with exponential decay, $N = 10$, $\epsilon = 5\% \cdot (n_{co} - n_{cl})$.

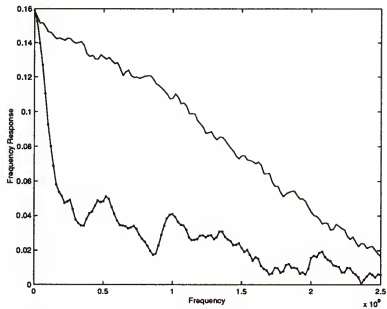


Figure 3.6: Frequency responses of the optimal profile (solid) and of the ripple distortion (dotted) with exponential decay, $N = 10$, $\epsilon = 5\% \cdot (n_{co} - n_{cl})$.

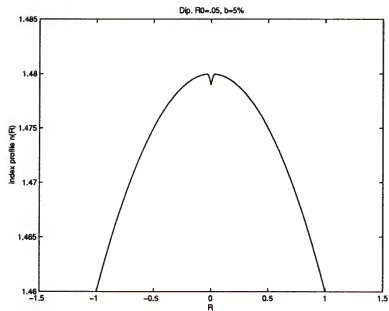


Figure 3.7: Dip distortion profile, $R_0 = .05$, $\epsilon = 5\%(n_{co} - n_{cl})$.

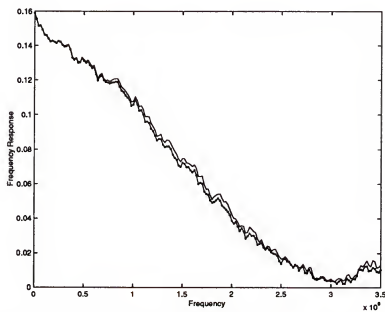


Figure 3.8: Frequency responses of the optimal profile (solid) and of the dip distortion, $R_0 = .05$, $b = 5\%(n_{co} - n_{cl})$.

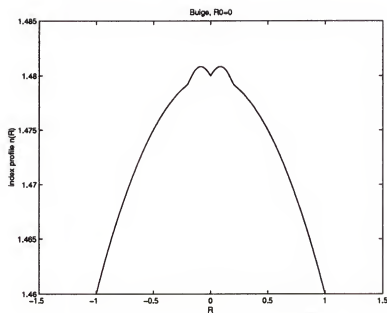


Figure 3.9: Bulge distortion, $R_0 = 0$.

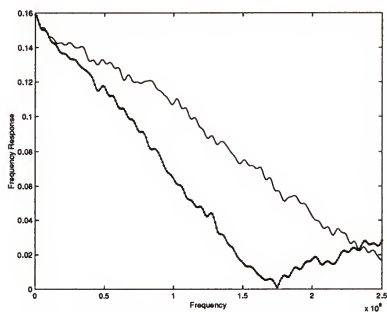


Figure 3.10: Frequency response of the optimal profile (solid) and of the bulge distortion (dotted), $R_0 = 0$.

Table 3.4: Bandwidths of Dip Distortions: $p(R) = n_{co}(1 - 2\Delta R^2)^{\frac{1}{2}} - b \cdot \exp\left(-\frac{R_0^2}{(R_0 - R)^2} + 1\right)$, $0 \leq R \leq R_0$.

b	R_0	$BD(MHz \cdot km)$
$5\% \cdot (n_{co} - n_{cl})$.05	1384
$5\% \cdot (n_{co} - n_{cl})$.10	1289
$10\% \cdot (n_{co} - n_{cl})$.05	1302
$10\% \cdot (n_{co} - n_{cl})$.10	1195
$15\% \cdot (n_{co} - n_{cl})$.05	1270
$15\% \cdot (n_{co} - n_{cl})$.10	1172
$20\% \cdot (n_{co} - n_{cl})$.05	1219
$20\% \cdot (n_{co} - n_{cl})$.10	1164

Table 3.5: Bandwidths of Bulge Distortions: $p(R) = \epsilon \sin\{5\pi(R - R_0)\}$, $R_0 \leq R \leq R_0 + 0.2$.

ϵ	R_0	$BD(MHz \cdot km)$
$5\% \cdot (n_{co} - n_{cl})$	0	888
$5\% \cdot (n_{co} - n_{cl})$.1	672
$5\% \cdot (n_{co} - n_{cl})$.2	562
$5\% \cdot (n_{co} - n_{cl})$.4	239
$5\% \cdot (n_{co} - n_{cl})$.6	138
$5\% \cdot (n_{co} - n_{cl})$.8	634

CHAPTER 4

A FINITE ELEMENT METHOD FOR CIRCULAR FIBERS

The propagating fields in a weakly guiding circular fiber are governed by the scalar wave equation which is a singular Sturm-Liouville eigenvalue problem on the unbounded interval $(0, \infty)$. The finite element method developed by Höhn [17], is generalized to solve the scalar wave equations.

4.1 Unbounded Domain or Non-Compact Problem

We recall that Maxwell's wave equations of electromagnetic fields in a weakly guiding circular fiber can be approximated by scalar wave equations by ignoring the polarization effects. We again assume that the index profile n is radially symmetric and longitudinal invariant. *i.e.*,

$$n^2(x, y, z) = \begin{cases} n^2(r) & 0 < r < a, \\ n_{cl}^2 & r \geq a \end{cases} \quad (4.1)$$

where a is the core radius, $n(r)$ is real-valued, bounded, piecewise continuous, and n_{cl} (a positive constant) is the refractive index in the cladding. Therefore, the cylindrical coordinates (r, θ, z) are used where z is the fiber axis. The longitudinal component of TE fields, denoted here as E_m , can be expressed as

$$E_m(r, \theta, z) = \begin{cases} \Psi_m(r) \cos(m\theta) \exp(-i\beta z) & \text{even mode} \\ \Psi_m(r) \sin(m\theta) \exp(-i\beta z) & \text{odd mode} \end{cases} \quad (4.2)$$

where β is the propagation constant, and $\Psi_m(r)$ is the solution of the scalar wave equation

$$u'' + \frac{u'}{r} + \left\{ k^2 n^2(r) - \frac{m^2}{r^2} \right\} u = \beta^2 u, \quad r \in (0, \infty) \quad (4.3)$$

where $k = 2\pi/\lambda$ is the wave number. This second-order differential equation is classically known as the *singular* Sturm-Liouville eigenvalue problem because of the unbounded domain and singularities at $r = 0$ and $r = \infty$. In the traditional finite element methods, the unbounded domain is truncated to a finite domain, i.e., $u(r) \equiv 0$, $\forall r \geq r_0 > 0$, and the finite dimensional spaces V_h are used to approximate the eigenfunctions. This truncation method works well provided that the eigenfunctions decay rapidly like $e^{-\alpha r}$ for $\alpha > 0$ sufficiently large. For $\alpha > 0$ small, the finite dimensional approximate spaces might perform poorly. The second disadvantage of this method is that if the original problem is of the non-compact case (e.g. Rellich-Gårding compact embedding condition [3], [19] does not hold), the approximating eigenvalues λ_h of the discrete problem (compact) might converge to a non-eigenvalue of the continuous problem [31]. This phenomenon is known as the existence of spurious solutions. Such non-compact differential operators on a bounded interval has been studied in [27] and on an unbounded interval in [17]. We now briefly describe the methods developed in [27] and [17]. Let H be a Hilbert space and $V \subset H$ a closed subspace. Consider the generalized eigenvalue equation

$$Lu = \lambda Mu \tag{4.4}$$

where $(L, D(L))$ and $(M, D(M))$ are differential operators with $D(L) \subset V$ and $D(M) \subset H$. Let $(L_h, D(L_h))$ be the corresponding differential operator for the discrete problem. Assume L and L_h are invertible with the inverses L^{-1} and L_h^{-1} , respectively. Denote $T := L^{-1}M$ and $T_h := L_h^{-1}M_h$. So the general eigenvalue problem is reduced to find eigenvalues of the bounded operators T and T_h . If the finite element subspaces are finite dimensional, T_h is finite rank, hence compact. The usual assumption of the norm (uniform) convergence [12] $\|T - T_h\| \rightarrow 0$ as $h \rightarrow 0$ excludes

the situation where T is non-compact. In [27], the eigenvalue problem is defined on a bounded interval and a weaker condition of strong convergence $\|Tu - T_h u\| \rightarrow 0$ instead of the norm convergence is assumed. As in the compact case, each isolated eigenvalue of T can be approximated by a sequence of eigenvalues of the compact operators T_h ; however, it is not true in general that every sequence of approximate eigenvalues will converge to an (isolated) eigenvalue of T . In [17], the eigenvalue problem is defined on an unbounded interval with singularities at the end-points. The approximate subspaces V_h are chosen to be infinite dimensional as follows. Let I be a bounded interval. On I , V_h consists of the usual finite element functions. Outside of I , V_h is identical to V . This method eliminates the two disadvantages mentioned above. However, it requires the fundamental set of solution(s) at each end-point to be known. In this chapter, we extend the result of this work to solve our scalar wave equation on $(0, \infty)$ where only the fundamental solution at infinity is available.

4.2 Variational Formulation for E_z Field

Let $H := L^2(0, \infty, r)$ be the Hilbert space equipped with the inner product

$$(u, v) := (u, v)_H := \int_0^\infty uvrdr, \quad (4.5)$$

and hence H -norm is defined as

$$\|u\| := \|u\|_H := \left(\int_0^\infty |u|^2 r dr \right)^{\frac{1}{2}}. \quad (4.6)$$

Consider the differential operator L

$$Lu := -\frac{1}{r}(ru')' + \left\{ \frac{m^2}{r^2} - k^2 n^2(r) \right\} u \quad (4.7)$$

with the domain $D(L) = \{u \in C^1(0, \infty) : Lu, u, u' \in H, \text{ and } \frac{u}{r^2} \in H \text{ if } m \neq 0\}$. Then the scalar wave equation can be expressed in terms of L as $(L + \beta^2)u = 0$.

Consider the following variational formulation

$$a(u, v) := \int_0^\infty u'v' r dr + \int_0^\infty \left\{ \frac{m^2}{r^2} - k^2 n^2(r) \right\} uvr dr = -\beta^2 \int_0^\infty uvr dr. \quad (4.8)$$

Let

$$V := \{u \in H : u' \in H, \lim_{r \rightarrow 0} \sqrt{r}u(r) = \lim_{r \rightarrow \infty} \sqrt{r}u(r) = 0\}. \quad (4.9)$$

V is a closed subspace of H , $\bar{V} = H$, and is equipped with the weighted norm

$$\|u\|_V = \left(\int_0^\infty (|u|^2 + |u'|^2) r dr \right)^{\frac{1}{2}}. \quad (4.10)$$

Proposition 4.2.1 *If $u \in V$, $\frac{u}{r} \in H$.*

Proof: First, we show the proposition for $u \in C^1(0, \infty) \cap V$, then by the density of C^1 in V we are done. Since $\lim_{r \rightarrow \infty} u(r) = 0$, we have

$$\frac{u(r)}{r} = -\frac{1}{r} \int_r^\infty u' dt.$$

Let

$$g(r) := \frac{1}{r} \int_r^\infty u'(t) \sqrt{t} dt.$$

Then by Hardy-Littlewood's inequality [10], we have

$$\int_0^\infty g^2 dr \leq 2 \int_0^\infty u'^2 r dr.$$

Using this inequality, we get

$$\begin{aligned} \int_0^\infty \frac{u^2}{r^2} r dr &= \int_0^\infty \frac{1}{r} \left\{ \int_r^\infty u' \frac{\sqrt{t}}{\sqrt{t}} dt \right\}^2 dr \\ &\leq \int_0^\infty \frac{1}{r^2} \left\{ \int_r^\infty u' \sqrt{t} dt \right\}^2 dr \\ &\leq 2 \int_0^\infty u'^2 r dr. \end{aligned} \quad (4.11)$$

Hence, $\left\| \frac{u}{r} \right\| \leq 2\|u'\| < \infty$. ■

Remark: The inequality (4.11) complements the well-known Hardy's inequality

$$\int_0^\infty r^\gamma |u|^2 dr \leq \frac{4}{(\gamma+1)^2} \int_0^\infty r^{\gamma+2} |u'|^2 dr, \quad \gamma \neq 1, \quad u \in C_0^\infty(0, \infty). \quad (4.12)$$

Therefore, $a(u, v)$ is a bilinear form defined on $V \times V$ for $m = 0, 1, 2, \dots$

Proposition 4.2.2 *The bilinear form $a(u, v)$ is symmetric, continuous on $V \times V$ and bounded from below by $-k^2 n_{max}^2$.*

Proof: Let $u, v \in V$. It is clear that $a(\cdot, \cdot)$ is symmetric. By Hölder's inequality we have

$$\begin{aligned} |a(u, v)| &\leq \int_0^\infty |u'v'|rdr + \int_0^\infty \left| \frac{m^2}{r^2} - k^2 n^2 \right| |uv|rdr \\ &\leq \|u'\| \|v'\| + m^2 \|u/r\| \|v/r\| + k^2 \|n^2\|_\infty \|u\| \|v\| \\ &\leq C(m) \|u\|_V \|v\|_V. \end{aligned}$$

Hence, $a(u, v)$ is continuous. Also,

$$\begin{aligned} a(u, u) &\geq \int_0^\infty |u'|^2 r dr + m^2 \int_0^\infty \frac{u^2}{r^2} r dr - k^2 n_{max}^2 \int_0^\infty |u|^2 r dr \\ &> -k^2 n_{max}^2 \|u\|^2. \end{aligned}$$

So, the bilinear form $a(\cdot, \cdot)$ is symmetric, and bounded from below by the constant $-k^2 n_{max}^2$. ■

Remark: If $\alpha > k^2 n_{max}^2$, the bilinear form

$$b(u, v) := a(u, v) + \alpha(u, v) \quad (4.13)$$

is continuous and V-elliptic. The space V with the inner product $b(u, v)$ is a Hilbert space.

By a representation theorem ([20], theorem VI.2.2.6), there exists a unique self-adjoint linear operator A with $D(A) \subset D(a) = V$ and

$$a(u, v) = (Au, v) \quad \forall u \in D(A), v \in V \quad \text{and} \quad (4.14)$$

$$(Au, u) \geq -k^2 n_{max}^2 \|u\|^2. \quad (4.15)$$

Proposition 4.2.3 *The spectrum of A , $\sigma(A)$, is a subset of the interval $[-k^2 n_{max}^2, \infty)$. The essential spectrum of A , $\sigma_{ess}(A)$ is the subinterval $[-k^2 n_{cl}^2, \infty)$.*

Proof: Since $A \geq -k^2 n_{max}^2$, $\sigma(A) \subset [-k^2 n_{max}^2, \infty)$.

By definition, $A = L$ on $D(L)$. By the transformation $w(r) = \sqrt{r}u(r)$, we obtain the differential equation

$$-w'' + \left(\frac{m^2 - \frac{1}{4}}{r^2} - k^2 n^2(r) \right) w = -\beta^2 w. \quad (4.16)$$

We have $\lim_{r \rightarrow \infty} \frac{m^2 - \frac{1}{4}}{r^2} - k^2 n^2(r) = -k^2 n_{cl}^2$. Hence, $\sigma_{ess}(A) = [-k^2 n_{cl}^2, \infty)$ [29]. ■

Remark: The propagation constants β of propagating modes must satisfy

$$kn_{cl} < \beta \leq kn_{max}.$$

For $\alpha > -k^2 n_{max}^2$, the non-homogeneous equation

$$(A + \alpha)u = f \quad (4.17)$$

has a unique solution $u \in D(A)$ for any $f \in H$, because $-\alpha$ is in the resolvent set $\rho(A)$. Hence, the resolvent of $A + \alpha$ exists and is bounded, denoted by

$$T := R_\alpha(A) := (A + \alpha)^{-1}.$$

The operator T is defined everywhere on H with the range $D(A)$. If μ is an eigenvalue of $A + \alpha$, $\lambda := \frac{1}{\mu} - \alpha$ is an eigenvalue of T . Hence, the problem of finding eigenvalues of

the differential operator $A + \alpha$ reduces to finding eigenvalues of the bounded operator (Green operator) T . The corresponding eigenfunctions of $A + \alpha$ and of T are identical.

Embeddings in weighted Sobolev spaces. The Hilbert space $H = L^2(0, \infty, r)$ is an example of a power-type weighted Sobolev space on $(0, \infty)$ [21]. Define

$$H^m(0, \infty, r) = \{\sqrt{r}u^{(j)} \in L^2(0, \infty), j = 0, 1, \dots, m\}. \quad (4.18)$$

Lemma 4.2.4 [21] *The set $\mathcal{A} = \{\phi \in C^\infty(0, \infty) : \lim_{r \rightarrow \infty} u(r) = 0\}$ is dense in $L^2(0, \infty, r)$.*

Corollary 4.2.5 *The set $\mathcal{B} = \{\phi \in C^\infty(0, \infty) : \lim_{r \rightarrow \infty} \sqrt{r}u(r) = 0\}$ is dense in $L^2(0, \infty, r)$.*

Lemma 4.2.6 [2] *If $u(r) \in C^1(0, d)$, $d < \infty$ and $u' \in L^1(0, d, r)$, then*

$$\lim_{r \rightarrow 0} \sqrt{r} u(r) = 0.$$

Corollary 4.2.7 *If $u(r) \in C^1(0, \infty)$ and $u' \in L^1(0, \infty, r)$, then*

$$\lim_{r \rightarrow 0} \sqrt{r} u(r) = 0.$$

Lemma 4.2.8 *Let $u(r) \in \mathcal{B}$ where \mathcal{B} is defined in corollary 4.2.5. Then*

$$\int_0^\infty |u|^2 dr \leq 2 \int_0^\infty |u||u'|r dr. \quad (4.19)$$

Proof: By integration by parts and corollary 4.2.7, we have

$$\int_0^\infty |u|^2 dr = -2 \int_0^\infty |u| \frac{d}{dr} |u(r)| r dr.$$

Thus,

$$\int_0^\infty |u|^2 dr \leq 2 \int_0^\infty |u||u'|r dr.$$

This completes the proof. ■

Corollary 4.2.9 *If $u \in H^1(0, \infty, r)$ then $u \in L^2(0, \infty)$ and*

$$\|u\|_{L^2(0, \infty)} \leq 2\|u'\|_{L^2(0, \infty, r)}. \quad (4.20)$$

Proof: The proof follows directly from the previous lemma. ■

Finally, for completeness, we state a lemma in [2].

Lemma 4.2.10 *Let $u \in C^1(0, d)$. If $p \geq 1$, $\nu > 0$, then*

$$\begin{aligned} \sup_{(0, d)} |u(r)|^p &\leq \frac{2}{d} \int_0^d |u|^p dr + \int_0^d |u|^{p-1} |u'| dr, \\ \sup_{(0, d)} r^\nu |u(r)|^p &\leq \frac{\nu + 3}{d} \int_0^d |u|^{p-1} r^\nu dr + 2p \int_0^d |u|^{p-1} |u'| r^\nu dr. \end{aligned}$$

Corollary 4.2.11 *If $u \in C^1(0, \infty)$, then*

$$\begin{aligned} \sup_{(0, \infty)} |u(r)|^2 &\leq \int_0^\infty |u| |u'| dr, \\ \sup_{(0, \infty)} |u(r)|^2 r &\leq 4 \int_0^\infty |u| |u'| r dr. \end{aligned}$$

4.3 Finite Element Approximations

Let V_h be a subspace of V , not necessarily finite dimensional. Let's denote H_h as the completion of V_h in H . By the representation theorem, for $a(u_h, v_h)$ defined on $V_h \times V_h$, there exists a unique self-adjoint operator A_h with $D(A_h) \subset V_h$ which is bounded from below by $-k^2 n_{max}^2$ and satisfies

$$(A_h u_h, v_h) = a(u_h, v_h), \quad \forall u_h \in D(A_h), v_h \in V_h. \quad (4.21)$$

A_h is not necessarily compact since V_h is not finite dimensional. The inverse of $A_h + \alpha$ exists and bounded in H_h for $\alpha > k^2 n_{max}^2$, denoted by T_h . This implies that for every $f \in H_h$, the unique solution of the non-homogeneous equation

$$(A_h + \alpha)u = f \quad (4.22)$$

is $u_h := T_h f$. Equivalently, the function u_h satisfies the variational equation

$$a(u_h, v_h) + \alpha(u_h, v_h) = (f, v_h), \quad \forall v_h \in V_h. \quad (4.23)$$

Remarks: There are three projections of V onto V_h that are useful for our purposes.

1. The orthogonal projection $P_h : H \mapsto V_h$ defined as follows. For each $f \in H$,

$$(P_h f, v_h) = (f, v_h), \quad \forall v_h \in V_h. \quad (4.24)$$

With this projection, we can extend the operator T_h to H by

$$T_h f := T_h P_h T, \quad \forall f \in H. \quad (4.25)$$

In fact, the solution $u_h := T_h f$ of the variational equation (4.23) remains the same for every $f \in H$.

2. The interpolating projection $\pi_h : H \mapsto S_h(I)$ where $S_h(I)$ is a finite dimensional (closed) subspace of V_h consisting of polynomials defined on a bounded interval I .

We will come back to S_h later.

3. The eigenspace projection $Q : H \mapsto N_l(\lambda_0) \subset V$.

Let $N_l(\lambda_0)$ be the subspace of generalized eigenfunctions of T associated with the eigenvalue λ_0 of (algebraic) multiplicity l . Let Γ be a simple closed curve about λ_0 such that the region bounded by Γ and containing λ_0 intersects with the spectrum of T only at λ_0 . The projection Q is defined by the Cauchy-type integral [20]

$$Q := -\frac{1}{2\pi i} \oint_{\Gamma} (T - \xi)^{-1} d\xi. \quad (4.26)$$

Hence, if λ_0 is an eigenvalue of T , $TQu = \lambda_0 Qu$, $\forall u \in H$. Similarly, we can also define the projection $Q_h : H \mapsto N_l(\lambda_0^h)$ where λ_0^h is an eigenvalue of the operator T_h .

We hope that $Q_h u \rightarrow Qu$ as $h \rightarrow 0$.

The subspaces V_h are assumed to satisfy the following approximation properties.

Approximation Properties of V_h

A1. $\|T - T_h\| \leq \gamma_h$ where $\lim_{h \rightarrow 0} \gamma_h = 0$ (i.e., uniform convergence).

A2. Let $\lambda_0 \neq 0$ be an isolated eigenvalue of T of multiplicity l . Define the *gap* between the eigenspace associated with λ_0 and V_h as [20]

$$\begin{aligned} \epsilon(h) &:= \sup_{\substack{u \in N_l(\lambda_0) \\ \|u\| \leq 1}} \text{dist}(u, V_h) \\ &:= \sup_{\substack{u \in N_l(\lambda_0) \\ \|u\| \leq 1}} \inf_{u_h \in V_h} \|u - u_h\|. \end{aligned} \quad (4.27)$$

In particular, if λ_0 is a simple eigenvalue of T and u_0 is the corresponding eigenfunction, then $\epsilon(h) = \text{dist}(u_0, V_h)$.

We assume that

$$\lim_{h \rightarrow 0} \epsilon(h) = 0. \quad (4.28)$$

The assumption (A1) means that for any $f \in H$ the solutions $u := Tf$ and $u_h := T_h f$ of the non-homogeneous problems $((A + \alpha)u, v) = (f, v)$ and $((A_h + \alpha)u_h, v_h) = (f, v_h)$ respectively, satisfy

$$\|u - u_h\| \leq \gamma_h. \quad (4.29)$$

In the next lemma, we consider the regularity of solutions $u \in D(A)$ of the equation $Au = f$, i.e.,

$$-u'' - \frac{u'}{r} - \left(k^2 n^2 - \frac{m^2}{r^2}\right)u = f, \quad 0 < r < \infty.$$

Lemma 4.3.1 *Let $f \in H$. If $u \in D(A)$ satisfies $Au = f$, then $u \in H^2(0, \infty, r)$.*

Proof: Let $u \in D(A)$ be a solution of

$$-u'' - \frac{u'}{r} - \left(k^2 n^2 - \frac{m^2}{r^2}\right)u = f, \quad 0 < r < \infty,$$

or, equivalently,

$$-(ru')' - \left(k^2 n^2 - \frac{m^2}{r^2}\right) u \cdot r = f \cdot r.$$

Since $\lim_{r \rightarrow 0} r \cdot u'(r) = 0$, we have

$$-u' = \frac{1}{r} \int_0^r \left(k^2 n^2(s) - \frac{m^2}{s^2}\right) u(s) s \, ds + \frac{1}{r} \int_0^r f(s) s \, ds.$$

Since $\lim_{r \rightarrow 0} \sqrt{r} \cdot u(r) = 0$, we further have

$$u = \int_r^\infty \frac{1}{t} \int_0^t \left(k^2 n^2(s) - \frac{m^2}{s^2}\right) u(s) s \, ds \, dt + \int_r^\infty \frac{1}{t} \int_0^t f(s) s \, ds \, dt.$$

By differentiating the integral representation of u twice, we obtain

$$u'' = \frac{1}{r^2} \int_0^r \left(k^2 n^2(s) - \frac{m^2}{s^2}\right) u(s) s \, ds - \left(k^2 n^2(s) - \frac{m^2}{r^2}\right) u(r) + \frac{1}{r^2} \int_0^r f(s) s \, ds - f(r).$$

Using Hardy-Littlewood's inequality, i.e.,

$$\left\| \frac{1}{x} \int_0^x f(s) s \, ds \right\|_{L^2(0, \infty)} \leq 2 \|f\|_{L^2(0, \infty)},$$

we obtain

$$\begin{aligned} \|\sqrt{r} u''\|_{L^2} &\leq \left\| \frac{1}{r} \int_0^r \left(k^2 n^2(s) - \frac{m^2}{s^2}\right) u(s) \sqrt{\frac{s}{r}} \sqrt{s} \, ds \right\|_{L^2} + \left\| \frac{1}{r} \int_0^r f(s) \sqrt{\frac{s}{r}} \sqrt{s} \, ds \right\|_{L^2} + \\ &\quad \left\| \left(k^2 n^2 - \frac{m^2}{r^2}\right) u \sqrt{r} \right\|_{L^2} + \|f \sqrt{r}\|_{L^2} \\ &\leq \left\| \frac{1}{r} \int_0^r \left(k^2 n^2(s) - \frac{m^2}{s^2}\right) u(s) \sqrt{s} \, ds \right\|_{L^2} + \left\| \frac{1}{r} \int_0^r f(s) \sqrt{s} \, ds \right\|_{L^2} + \\ &\quad \left\| \left(k^2 n^2 - \frac{m^2}{r^2}\right) u \sqrt{r} \right\|_{L^2} + \|f \sqrt{r}\|_{L^2} \\ &\leq C(\|u \sqrt{r}\|_{L^2} + \|\frac{u}{r^2} \sqrt{r}\|_{L^2} + \|f \sqrt{r}\|_{L^2}). \end{aligned}$$

Since $u \in D(A)$, $\|\sqrt{r} u''\|_{L^2} < \infty$. ■

4.4 Convergence of Eigenvalues and Eigenfunctions

First, we restate the convergence results of the approximate eigenvalues and their corresponding eigenfunctions. From now on we assume that $\|T - T_h\| \rightarrow 0$ as $h \rightarrow 0$.

Lemma 4.4.1 *Let λ_0 be an isolated eigenvalue of the self-adjoint operator T with multiplicity l . Then for each $\epsilon > 0$ there exists $h_0(\epsilon) > 0$ such that for any $h < h_0(\epsilon)$ the spectrum of the self-adjoint T_h consists of l eigenvalues λ_h^i (counting multiplicity) and they satisfy*

$$|\lambda_h^i - \lambda| < \epsilon, \quad i = 1, 2, \dots$$

Proof: This is a well-known result in ([20], IV§3.4). ■

Lemma 4.4.2 *Let λ_h be a sequence of isolated eigenvalues of T_h converging to λ . Then λ is either an isolated eigenvalue of T or $-k^2 n_{cl}^2$.*

Proof: Since T and T_h are self-adjoint bounded operators, by ([20], V §4, theorem 4.10)

$$\begin{aligned} \sup_{\lambda_h \in \sigma(T_h)} \text{dist}(\lambda_h, \sigma(T)) &< \|T - T_h\|, \\ \sup_{\lambda \in \sigma(T)} \text{dist}(\lambda, \sigma(T_h)) &< \|T - T_h\|. \end{aligned}$$

So, if λ were in the resolvent set of T , there exist $\gamma > 0$ such that $\text{dist}(\lambda, \sigma(T)) \geq \gamma$. However, $\|T - T_h\| \rightarrow 0$, there is $h_0 > 0$ such that $\text{dist}(\lambda_{h_0}, \sigma(T)) < \gamma/4$ and $\sup_{h < h_0} |\lambda_h - \lambda| < \gamma/4$. Thus, it is a contradiction. If λ is a point in the essential spectrum of T , it has to be the point $-k^2 n_{cl}^2$ because $\sigma_{ess}(T) = [-k^2 n_{cl}^2, \infty)$. ■

Lemma 4.4.3 *Let λ be an isolated eigenvalue of T of multiplicity l . Let $\{\lambda_h\}$ be a sequence of eigenvalues of T_h such that $\lim_{h \rightarrow 0} \lambda_h = \lambda$ and $\{u_h\} \subset V_h$ be the*

sequence of the associated eigenfunctions. Then there exists a subsequence of $\{u_h\}$ that converges to $u \in V$, $u \neq 0$, and u is an eigenfunction of T .

Proof: Let Γ be a simple closed curve containing λ in its interior and no other points of the spectrum of T . Let D be the region enclosed by Γ . For h small enough, there are l eigenvalues λ_h of T_h (counting multiplicity) such that they are all in D . Hence, the difference of the eigenprojections Q and Q_h can be written as

$$Q - Q_h = -\frac{1}{2\pi i} \oint_{\Gamma} (R_{\xi}(T) - R_{\xi}(T_h)) d\xi. \quad (4.30)$$

Therefore,

$$\begin{aligned} \|Q - Q_h\| &\leq \frac{1}{2\pi} \oint_{\Gamma} \|R_{\xi}(T) - R_{\xi}(T_h)\| |d\xi| \\ &\leq \frac{1}{2\pi} \oint_{\Gamma} \|R_{\xi}(T)\| \|T - T_h\| \|R_{\xi}(T_h)\| |d\xi|. \end{aligned}$$

Since the curve Γ is compact and $R_{\xi}(T)$, $R_{\xi}(T_h)$ are continuous functions on the resolvent sets of T and T_h , respectively, we conclude that $\|Q - Q_h\| \rightarrow 0$ for $\|T - T_h\| \rightarrow 0$. Hence, $\|Q u - Q_h u\| \rightarrow 0$, $\forall u \in H$. Therefore, there is a subsequence in $\{Q_h u\}$, denoted by u_h , that converges to an eigenfunction $u \in \{Q u\}$. ■

Remark: In the above proof, we can see that if $\|T - T_h\| \leq \gamma_h$ then $\|Q - Q_h\| \leq C \gamma_h$.

This gives us the convergence rate of the eigenfunctions.

The next theorem is proved in [27].

Theorem 4.4.4 *Let λ_0 be an isolated eigenvalue of T with eigenfunction u_0 . Let $\{\lambda_h\}$ be a sequence of eigenvalues of T_h such that $\lambda_h \rightarrow \lambda_0$ and $\{u_h\} \subset V_h$ the corresponding eigenfunctions that converges to u_0 . Then the rates of the convergence are*

$$|\lambda_h - \lambda_0| \leq C \epsilon(h)^2, \quad (4.31)$$

$$\|u_h - u\|_H \leq C \epsilon(h), \quad (4.32)$$

for sufficiently small h , where the gap $\epsilon(h)$ depends on the choice of the approximate subspaces V_h .

4.5 The Subspaces V_h

Let $I := [0, a]$ where a is the core radius. We define the approximate spaces V_h as follows. Let \mathcal{P} be a partition of the closed interval $I := [0, a]$ defined by $0 = x_0 < x_1 < \dots < x_N = a$. Set

$$\begin{aligned} h_i &:= x_i - x_{i-1}, \\ h &:= \max_i h_i, \\ \tau &:= \frac{\min_i h_i}{h}. \end{aligned}$$

Let S_h be the finite dimensional space of continuous functions which are polynomials of degree 1 on each subinterval $I_i := (x_{i-1}, x_i)$, $i = 1, 2, \dots, N$. Define

$$V_h := \{v \in V : v|_{(0, a)} \in S_h\}. \quad (4.33)$$

Thus, V_h consists of functions in V outside the interval $(0, a)$. So, V_h is infinite dimensional, thus the essential spectrum of T_h might not be empty.

We now show that the essential spectrums of T and of T_h are identical. This can be accomplished if we can show that the difference $T - T_h$ is a compact operator [20].

Lemma 4.5.1 *$T - T_h$ is compact.*

Proof: We want to show that for any bounded sequence in H , there exists a subsequence whose image under $T - T_h$ is a convergent sequence. We consider $T - T_h$ on two subintervals $(0, a)$ and (a, ∞) .

1. Let $f_n \in H$ with $\|f_n\| = 1$, $n = 1, 2, \dots$

We want to show that the sequence $\{(T - T_h)f_n\}$ is precompact in H , i.e., there exists a subsequence that converges (strongly) in H . Denote

$$\begin{aligned} u_n &:= T f_n \\ u_{h_n} &:= T_h f_n, \quad n = 1, 2, \dots \end{aligned}$$

On the unbounded subinterval (a, ∞) , u_n and u_{h_n} are both in the same space V , and they both solve the non-homogeneous equation (4.17). Hence, the difference $w_n := u_n - u_{h_n}$ satisfies the modified Bessel equation

$$-\frac{1}{r}(r w_n')' + (\alpha - k^2 n_{cl}^2) w_n + \frac{m^2}{r^2} w_n = 0, \quad (a, \infty).$$

Since this equation is of the limit-point at infinity, there is only one fundamental solution which is denoted by

$$u_a(r) = K_m \left(\sqrt{\alpha^2 - k^2 n_{cl}^2} r \right).$$

Therefore, $w_n(r)$ must be a constant multiple of $u_a(r)$, i.e.,

$$w_n(r) = c_n u_a(r), \quad r \geq a. \quad (4.34)$$

2. By the proposition 4.2.2, for every n ,

$$\begin{aligned} \|u_n\|_{H^1(0, \infty, r)}^2 &\leq ((A + \alpha)u_n, u_n) = (f_n, u_n) \\ &\leq \|f_n\| \|u_n\| \quad (\|\cdot\| \text{ norm in } H) \\ &= \|f_n\| \|T f_n\| \\ &\leq \|f_n\|^2 \|T\| = \|T\| \quad (\|f_n\| = 1). \end{aligned}$$

Therefore, on the subinterval $(0, a)$, we obviously have $\|u_n\|_{H^1(0, a, r)}^2 \leq \|T\|$ for each n . Similarly, $\|u_{h_n}\|_{H^1(0, a, r)}^2 \leq \|T_h\|$. Hence,

$$\|w_n\|_{H^1(0, a, r)} = \|u_n - u_{h_n}\|_{H^1(0, a, r)} \leq 2\|T\|. \quad (4.35)$$

3. Here we show that the constants c_n in (4.34) are bounded. We have

$$\int_a^\infty (A + \alpha)(u_n - u_{h_n})(u_n - u_{h_n})rdr = 0. \quad (4.36)$$

Integrating (4.36) by parts and since $u_a(r) > 0$, $u'_a(r) < 0$, we have

$$\begin{aligned} \int_a^\infty w_n^2 r dr + \int_a^\infty (\alpha - k^2 n_{cl}^2) w_n^2 r dr + m^2 \int_a^\infty \frac{w_n^2}{r} dr &= -ac_n^2 u'_a(a) u_a(a) \\ &= ac_n^2 |u'_a(a) u_a(a)|. \end{aligned} \quad (4.37)$$

However, from (4.35), we get

$$c_n^2 \leq \frac{2\|T\|}{a|u'_a(a)u_a(a)|}. \quad (4.38)$$

4. Finally, by (4.35), w_n is a bounded sequence in $H^1(0, a, r)$. For bounded interval $(0, a)$, $H^1(0, a, r)$ is compactly embedded in $L^2(0, a, r)$. Hence, there exists a subsequence of $\{w_n\}$, labeled again by $\{w_n\}$, that converges in $L^2(0, a, r)$ to, say $w \in L^2(0, a, r)$. For this sequence, we also have

$$\sup_n |w_n(r)| = \sup_n |c_n| |u_a(r)| \leq C |u_a(r)| \quad \forall r \in (a, \infty).$$

Hence, we pick a subsequence of $\{c_n\}$ such that $c_n \rightarrow c_0$, so

$$|u_n(r) - u_{h_n}(r)| = |w_n(r)| \xrightarrow{n} |w(r)| \quad \text{in } L^2(0, a, r), \quad (4.39)$$

$$|u_n(r) - u_{h_n}(r)| = |w_n(r)| \xrightarrow{n} c_0 |u_a(r)| \quad \forall r \in (a, \infty). \quad (4.40)$$

These imply that $\{w_n\}$ contains a subsequence that converges in H , i.e., $(T - T_h)u_n$ consists of a convergent subsequence in H . Thus, $T - T_h$ is compact as desired. ■

Now we show that $\|T - T_h\| \leq Ch^s$ for some $s > 0$ for V_h chosen above. On the subintervals I_i , $i = 1, 2, \dots, N$, the standard approximation theory applies. For the interval $I_0 = (0, x_1)$ that contains the singularity $x_0 = 0$, we need a Poincaré-type inequality.

Lemma 4.5.2 *Let $u \in H^1(0, h, r)$ with $u(h) = 0$. Then*

$$\int_0^h u^2 r dr \leq h \int_0^h (u')^2 r dr. \quad (4.41)$$

Proof: As usual, we first show that the inequality holds for functions in $C^1(0, h]$.

Then by completion, it holds for functions in $H^1(0, h, r)$. If $u(h) = 0$, we see that

$$\begin{aligned} |\sqrt{r}u(r)| &= |\sqrt{r} \int_r^h u(t)' dt| \\ &\leq |\int_r^h \sqrt{t} u'(t) dt| \\ &\leq \int_0^h \sqrt{t} |u'(t)| dt = \|\sqrt{r}u'\|_{L^1(0, h)}. \end{aligned}$$

This and Cauchy-Schwartz inequality imply that

$$\begin{aligned} \int_0^h |u|^2 r dr &\leq h \|\sqrt{r}u\|_{L^\infty(0, h)}^2 \\ &\leq h \|\sqrt{r}u'\|_{L^1(0, h)}^2 \\ &\leq h^2 \|\sqrt{r}u'\|_{L^2(0, h)}^2. \end{aligned}$$

Hence, the Poincaré-type inequality holds. ■

Lemma 4.5.3 *For each $u \in V$, there exist a constant $C = C(h, \rho)$ and $w \in V_h$ such that*

$$\|u' - w'\|_{L^2(0, a, r)} \leq Ch \|u''\|_{L^2(0, a, r)} \quad (4.42)$$

where h, ρ are defined in the beginning of the section.

Proof: Let $w(r)$ be a linear polynomial on I_0 with $w(x_1) = u(x_1)$ and $w'(x_1) = u'(x_1)$.

Applying lemma 4.5.2 to the difference $u'(r) - w'(r)$, we get

$$\int_0^h |u' - w'|^2 r dr \leq h^2 \int_0^h |u''|^2 r dr.$$

On each I_i , $i > 1$, let $w(r)$ interpolate $u(r)$ at end points $\{x_{i-1}, x_i\}$. This type of interpolant is known to satisfy [12]

$$\|u' - w'\|_{L^2(I_i)} \leq h \|u''\|_{L^2(I_i)}. \quad (4.43)$$

So,

$$\begin{aligned} \|u' - w'\|_{L^2(I_i, r)}^2 &:= \int_{x_{i-1}}^{x_i} (u' - w')^2 r dr \\ &\leq x_i \int_{x_{i-1}}^{x_i} (u' - w')^2 dr \\ &\leq x_i h_i^2 \int_{x_{i-1}}^{x_i} (u'')^2 dr \\ &\leq x_i h_i^2 \frac{1}{x_{i-1}} \int_{x_{i-1}}^{x_i} (u'')^2 r dr \\ &\leq C(h, \rho) h^2 \|u''\|_{L^2(I_i, r)}, \quad i = 2, 3, \dots \end{aligned}$$

Now, summing over i , we get

$$\|u' - w'\|_{L^2(0, a, r)} \leq Ch \|u''\|_{L^2(0, a, r)}. \quad (4.44)$$

This completes the proof. ■

Now we are ready to prove the error estimate for the non-homogeneous problem.

Recall that the symmetric V -elliptic and continuous bilinear form $b(u, v)$ is defined as

$$b(u, v) := a(u, v) + \alpha(u, v) := \int_0^\infty u' v' r dr + \int_0^\infty \left\{ \frac{m^2}{r^2} - k^2 n^2(r) + \alpha \right\} u v r dr.$$

Theorem 4.5.4 *Let $u \in V$ and $u_h \in V_h$ be the solutions of the non-homogeneous equations*

$$\begin{aligned} b(u, v) &= (f, v) \quad \forall v \in V, \\ b(u_h, v_h) &= (f, v_h) \quad \forall v_h \in V_h, \end{aligned}$$

where $f \in H$

$$\|u - u_h\|_V \leq C(h, \rho) h \|u''\|_H, \quad (4.45)$$

$$\|u - u_h\|_H \leq C(h, \rho) h^2 \|u''\|_H. \quad (4.46)$$

Proof: By the well-known Céa's lemma [6], we obtain

$$\begin{aligned} & b(u - u_h, u - u_h) \\ &= C \inf_{v_h \in V_h} b(u - v_h, u - v_h) \\ &= C \inf_{v_h \in V_h} \int_0^\infty \left\{ (u' - v_h')^2 + \left(\frac{m^2}{r^2} - k^2 n^2(r) + \alpha \right) (u - v_h)^2 \right\} r dr. \end{aligned} \quad (4.47)$$

There are two cases:

(i) $m = 0$. In this case, the coefficients of $b(u, v)$ are bounded, i.e., $0 < k^2 n^2(r) \leq k^2 n_{\max}^2 < \alpha$.

(ii) $m \neq 0$. In this case, we have seen in the proposition (4.2.1) that

$$\int_0^\infty \frac{m^2}{r^2} (u - v_h)^2 r dr < 2 \cdot m^2 \int_0^\infty (u' - v_h')^2 r dr < \infty.$$

Hence, by the definition of the subspace V_h ($V_h \equiv V$ on (a, ∞)), the remark above, and lemma 4.5.3, there exists $w \in V_h$ such that the infimum on the right side of (4.47) can be reduced to

$$\begin{aligned} b(u - u_h, u - u_h) &\leq C \inf_{v_h \in V_h} \int_0^a \left\{ (1 + 2m^2)(u' - v_h')^2 + (\alpha - k^2 n^2(r))(u - v_h)^2 \right\} r dr \\ &\leq C \int_0^a \left\{ (1 + 2m^2)(u' - w')^2 + (\alpha - k^2 n^2(r))(u - w)^2 \right\} r dr \\ &\leq C(h, \rho, m^2, \alpha) \left\{ h^2 \|u''\|_{L^2(0, a, r)}^2 + h^4 \|u''\|_{L^2(0, a, r)}^2 \right\}. \end{aligned}$$

Therefore,

$$b(u - u_h, u - u_h) \leq C(h, \rho, m^2, \alpha) h^2 \|u''\|_{L^2(0, a, r)}^2.$$

The continuity of the bilinear form also yields

$$\begin{aligned} \|u - u_h\|_V &\leq C \cdot b(u - u_h, u - u_h)^{\frac{1}{2}} \\ &\leq C(h, \rho, m^2, \alpha) h \|u''\|_{L^2(0,a,r)}. \end{aligned} \quad (4.48)$$

This proves the first part of the theorem. For the H -norm, we use *Aubin-Nitsche's duality argument* [6]. Since $V \subset H$ is dense in H , we have

$$\|u - u_h\|_H \leq M \|u - u_h\|_V \sup_{g \in H} \inf_{\psi_h \in V_h} \frac{\|\psi_g - \psi_h\|_V}{\|g\|_H}$$

where for any $g \in H$, $\psi_g \in V$ is the unique solution of $b(v, \psi_g) = (g, v)_H$. Using the similar argument as above, we can easily find that

$$\begin{aligned} \inf_{\psi_h \in V_h} \|\psi_g - \psi_h\|_V &\leq \inf_{\psi_h \in V_h} b(\psi_g - \psi_h, \psi_g - \psi_h) \\ &\leq C(m^2) \int_0^a (\psi_g' - w')^2 r dr + \int_0^a (\alpha - k^2 n^2) (\psi_g - w)^2 r dr \\ &\leq C(h, \rho, m^2, \alpha) \left\{ h^2 \|\psi_g''\|_{L^2(0,a,r)}^2 + h^4 \|\psi_g''\|_{L^2(0,a,r)}^2 \right\} \\ &\leq C(h, \rho, m^2, \alpha) h^2 \|\psi_g''\|_{L^2(0,a,r)}^2 \\ &\leq C(h, \rho, m^2, \alpha) h^2 \|g\|_H \quad \text{by lemma 4.3.1.} \end{aligned}$$

Thus, combining this inequality with (4.48), we finally have

$$\|u - u_h\|_H \leq M h^2 \|u''\|_{L^2(0,a,r)}.$$

This completes the proof. ■

Since $u = Tf$ and $u_h = T_h f$, we just show that with this particular choice of V_h ,

$$\|(T - T_h)f\|_H = \mathcal{O}(h^2), \quad \|(T - T_h)f\|_V = \mathcal{O}(h) \quad \forall f \in H \quad (4.49)$$

$$\text{hence, } \|T - T_h\| = \mathcal{O}(h). \quad (4.50)$$

So, by the theorem 4.4.4, the rate of convergence of the eigenfunctions is $\mathcal{O}(h)$ and that of the eigenvalues is $\mathcal{O}(h^2)$ since the gap $\epsilon(h) \leq \|T - T_h\|$ by definition.

4.6 Numerical Experiments

We use the V_h construct in the previous section to compute the propagating fields in circular fiber. We now consider the discretization of (4.8). Since we know the fundamental solution outside of the interval $(0, a)$, by integration by parts, the solution u_h of the variational formulation satisfies

$$b(u_h, v_h) - \lambda(u_h, v_h) = 0 \quad (4.51)$$

where

$$b(u_h, v_h) := \int_0^a u'_h v'_h x dx + \int_0^a \left(\alpha - k^2 n^2 + \frac{m^2}{x^2} \right) u_h v_h x dx - a c_a u'_a(a) v_h(a), \quad (4.52)$$

and $u_a(x) = K_m(Wx/a)$, and $\lambda = \alpha - \beta^2$.

The finite dimensional S_h has a basis $\{\psi_j\}_{j=1,2,\dots,N}$ where

$$\psi_0(x) = \frac{(x - x_1)}{(x_0 - x_1)}, \quad x \in (0, x_1), \text{ if } m = 0 \text{ (see the next remark for } m \geq 1),$$

for $1 \leq j \leq N-1$,

$$\psi_j(x) = \begin{cases} \frac{(x - x_{j-1})}{(x_j - x_{j-1})} & x \in (x_{j-1}, x_j), \\ \frac{(x - x_{j+1})}{(x_j - x_{j+1})} & x \in (x_j, x_{j+1}), \end{cases}$$

and

$$\psi_N(x) = \frac{(x - x_N)}{(x_N - x_{N-1})} \quad x \in (x_{N-1}, x_N).$$

Remark: If $m \geq 1$, the function ψ_0 is excluded from the basis of the approximating subspaces since $u(0) = 0$.

Then, each $u_h \in S_h$ can be expressed as

$$u_h = \sum_{j=1}^N u_j \psi_j \quad \text{where } u_j = u_h(x_j). \quad (4.53)$$

Denote the matrix $A = (a_{ij})$ where

$$a_{ij} = \int \psi'_i(x) \psi'_j(x) x dx + \int (\alpha - k^2 n^2(x)) \psi_i(x) \psi_j(x) x dx \quad (4.54)$$

and the matrix $B_0 = (b_{ij})$ where

$$b_{ij} = \int \psi_i(x) \psi_j(x) x dx. \quad (4.55)$$

Denote $U = (u_j)$. Then the matrix formulation of (4.51) is

$$AU - \lambda B_0 U + (0, \dots, a c_a u'_a(a))^T = 0. \quad (4.56)$$

Eigenfunctions u_h and their derivatives u'_h are continuous on $(0, \infty)$, so $u_N := u_h(x_N) = u_h(a) = c_a u_a(a) = c_a K_m(W)$. Hence, the constant c_a is

$$c_a = \frac{u_N}{u_a(a)}.$$

Substituting this in (4.55), we get

$$(A - B(\lambda))U = 0$$

$$\text{where } B(\lambda) := \lambda B_0 - \text{diag}(0, \dots, f(\lambda))$$

$$\text{with } f(\lambda) = a \frac{u'_a(a)}{u_a(a)} = a \frac{K'_m(W)}{K_m(W)}$$

$$\text{with } W = a \sqrt{\alpha - \lambda - k^2 n_{cl}^2}.$$

Therefore, our task is to solve for the eigenvector U and the eigenvalue λ . For this, we apply the inversion algorithm with shift strategy as in [17].

Algorithm: Let A and $B(\lambda)$ be Hermitian in a neighborhood \mathcal{U}_ϵ of λ_0 where λ_0 is an isolated eigenvalue of $(A - B(\lambda))U = 0$. Assume that the derivative $B'(\lambda)$ is positive definite in \mathcal{U}_ϵ . Given $\lambda_h \in \mathcal{U}_\epsilon$ and U_h with $\lambda_h \neq \lambda_0$ and $U_h^H B'(\lambda_0) U_0 \neq 0$. Define

$$(A - B(\lambda_h))V := B'(\lambda_h)U_h, \quad (4.57)$$

$$\lambda_{h+1} := \lambda_h + \frac{V^H B'(\lambda_h) U_h}{V^H B'(\lambda_h) V} \quad (4.58)$$

$$U_{h+1} := \frac{V}{\|V\|}. \quad (4.59)$$

Then for sufficiently small ϵ , $\lambda_h \rightarrow \lambda_0$ of order $\mathcal{O}(h^2)$ and $U_h \rightarrow U_0$.

Example: Since exact solutions for the circular fiber with truncated parabolic index profile are possible, we can check the accuracy of our finite element solutions. We recall that the truncated parabolic profile $n(r)$ is defined by

$$n^2(r) = \begin{cases} n_{co}^2 \left(1 - 2\Delta \frac{r^2}{a^2}\right) & 0 < r < a, \\ n_{cl}^2 & r \geq a, \end{cases}$$

where

$$\begin{aligned} n_{co} &= 1.48\mu\text{m}, \quad n_{cl} = 1.46\mu\text{m}, \quad a = 31.25\mu\text{m}, \\ \lambda &= 0.85\mu\text{m}(\text{wavelength}), \quad \Delta := \frac{1}{2} \left(1 - \frac{n_{cl}^2}{n_{co}^2}\right). \end{aligned}$$

In chapter 3, we have seen that the exact solutions for TE case are in terms of the Whittaker functions. The propagation constants are found by solving the eigenvalue equation

$$2V \frac{M'_{\kappa,\mu}(V)}{M_{\kappa,\mu}(V)} - 1 = W \frac{K'_m(W)}{K_m(W)} \quad (4.60)$$

where $M_{\kappa,\mu}(z)$ is the Whittaker function and

$$\begin{aligned} V &= ak\sqrt{n_{co}^2 - n_{cl}^2}, \quad U = a\sqrt{k^2 n_{co}^2 - \beta^2}, \quad W = a\sqrt{\beta^2 - k^2 n_{cl}^2}, \\ \kappa &= \frac{U^2}{4V}, \quad \mu = \frac{m}{2}. \end{aligned}$$

The first two largest propagation constants β for $m = 0, 1$ are computed by the finite element method. They are compared to the exact eigenvalues found in (4.60). The corresponding modes are well confined inside the core of radius a . The following tables are self-explanatory.

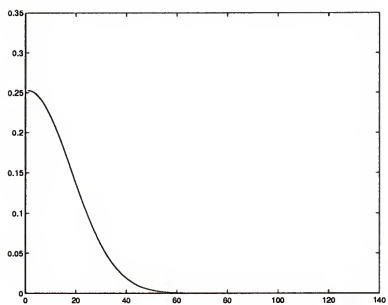


Figure 4.1: First mode for $m = 0, h = a/128$

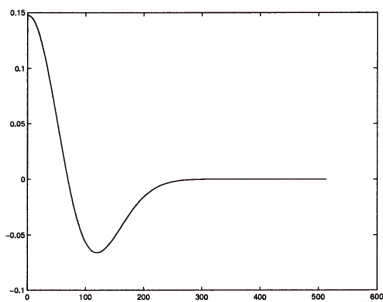


Figure 4.2: Second mode for $m = 0, h = a/512$

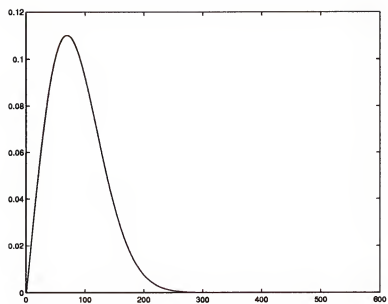


Figure 4.3: First mode for $m = 1, h = a/512$

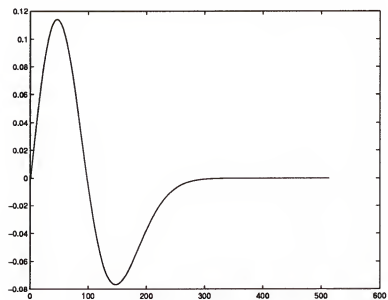


Figure 4.4: Second mode for $m = 1, h = a/512$

Table 4.1: Approximations of the largest β for $m = 0$.

N	Finite element	Error	Rate	Exact
8	10.9347148	1.7e-4		
16	10.9348452	4.5e-5	1.323	
32	10.9348785	1.2e-5	1.907	
64	10.9348872	2.9e-6	2.048	
128	10.9348894	7.0e-7	1.421	
256	10.9348900	1.0e-7	1.946	
512	10.9348901	2.5e-8	2.000	10.9348901

Table 4.2: Approximations of the second β for $m = 0$.

N	Finite element	Error	Rate	Exact
8	10.9228920	1.5e-3		
16	10.9239979	4.0e-4	1.901	
32	10.9242895	1.0e-4	2.000	
64	10.9243675	2.7e-5	1.889	
128	10.9243874	6.8e-6	1.989	
256	10.9243925	1.7e-6	2.000	
512	10.9243937	5.0e-7	1.765	10.9243942

Table 4.3: Approximations of the largest β for $m = 1$.

N	Finite element	Error	Rate	Exact
8	10.9293260	3.2e-4		
16	10.9298407	1.9e-4	0.752	
32	10.9297378	9.4e-5	1.015	
64	10.9296700	2.6e-5	1.854	
128	10.9296502	6.4e-6	2.022	
256	10.9296451	1.3e-6	2.299	
512	10.9296438	3.0e-7	2.115	10.9296438

Table 4.4: Approximations of the second β for $m = 1$.

N	Finite element	Error	Rate	Exact
8	10.9164070	2.7e-3		
16	10.9187833	3.6e-4	2.906	
32	10.9191934	5.1e-5	2.819	
64	10.9191672	2.5e-5	1.028	
128	10.9191491	6.7e-6	1.899	
256	10.9191441	1.7e-6	1.979	
512	10.9191428	4.0e-7	2.086	10.9191424

Table 4.5: Error in weighted L^2 -norm, $m = 0$.

N	Error	Rate
128	.0172	
256	.0073	1.231
512	.0030	1.274
1024	.0012	1.304
2048	.0004	1.328
4096	.0001	1.346

Table 4.6: Error in L^2 -norm, $m = 0$.

N	Error	Rate
128	.0096	
256	.0042	1.201
512	.0017	1.251
1024	.0007	1.286
2048	.0002	1.313
4096	.0001	1.334

CHAPTER 5 NON-CIRCULAR FIBERS AND DTN MAPS

In this chapter, we consider weakly guiding fibers with arbitrary core, *i.e.*, not necessarily circular. Hence, we need to solve Helmholtz eigenvalue equations governing the guided modes for the whole plane \mathbb{R}^2 . Combining the standard finite element method and Dirichlet-to-Neumann map (DtN), we can reduce the unbounded computational domain to a bounded one, in particular, to a circular disk of radius R . We use this method to study the propagating evanescent wave energy that exists outside the core of the square and circular fibers.

5.1 Dirichlet-to-Neumann Map

Since the geometry of the core is not circular, polar coordinate transformation is no longer helpful as in Chapter 3 and Chapter 4. We now consider the 2D scalar Helmholtz equations for the longitudinal components E_z and H_z of the electric and magnetic fields of propagating waves in the fiber:

$$(P_0) \quad \begin{cases} \Delta E_z + (k^2 n^2 - \beta^2) E_z = 0 & \text{in } \mathbb{R}^2, \\ E_z, \frac{\partial E_z}{\partial n} & \text{are continuous,} \\ E_z \in L^2(\mathbb{R}^2) \end{cases} \quad (5.1)$$

and

$$\begin{cases} \Delta H_z + (k^2 n^2 - \beta) H_z = 0 & \text{in } \mathbb{R}^2, \\ H_z, \frac{1}{n^2} \frac{\partial H_z}{\partial n} & \text{are continuous,} \\ H_z \in L^2(\mathbb{R}^2). \end{cases} \quad (5.2)$$

To ease the notation, we denote $u = E_z$ or H_z . The variational formulation of (5.1) is

$$a(u, v) := - \int_{\mathbb{R}^2} \nabla u \cdot \nabla v \, dxdy + \int_{\mathbb{R}^2} k^2 n^2 uv \, dxdy = \beta^2 \int_{\mathbb{R}^2} uv \, dxdy \quad (5.3)$$

and that of (5.2) is

$$a(u, v) := \int_{\mathbb{R}^2} \frac{1}{n^2} \nabla u \cdot \nabla v \, dxdy + \beta^2 \int_{\mathbb{R}^2} \frac{1}{n^2} uv \, dxdy = k^2 \int_{\mathbb{R}^2} uv \, dxdy \quad (5.4)$$

Remark: In the variational formulation of H_z , k^2 plays the role of eigenvalue.

We concentrate on the problem of E_z , the H_z problem can be treated identically. If we discretize (5.3), we face the difficulty of the unbounded domain. One of the widely-used techniques is to use compact-support finite elements to approximate the unbounded discrete problem. This is known to produce many spurious solutions. We hence adapt a method known as Dirichlet-to-Neumann map used in exterior and scattering problems. We show later that this method eliminates the undesired solutions. There are three main steps in using DtN methods. First, an appropriate artificial boundary Γ_R needs to be introduced so that its interior contains the core region Ω . Second, a boundary condition associated with Γ_R has to be determined in such a way that a Dirichlet condition is related to a Neumann condition. Third, a new reduced "interior" problem needs to be solved.

(i) *Artificial boundary Γ_R :* A natural choice for Γ_R is a circle of radius R where R is sufficiently large so that Ω is contained in the interior of Γ_R . The reason of this choice will be clear later.

(ii) *The DtN map:* Let's denote

$$\Omega_i := B_R \quad \text{the disk of radius } R\text{-the interior domain}$$

and

$$\Omega_e = \mathbb{R}^2 \setminus B_R \quad \text{the exterior domain.}$$

Hence, the Helmholtz problem in (5.1) is equivalent to the following eigenvalue problem:

Let $u_i := u|_{\Omega_i}$ and $u_e = u|_{\Omega_e}$. Then

$$\begin{cases} \Delta u_i + (k^2 n^2 - \beta^2) u_i = 0 & \text{in } \Omega_i, \\ \Delta u_e + (k^2 n^2 - \beta^2) u_e = 0 & \text{in } \Omega_e, \\ u_i = u_e & \text{on } \Gamma_R, \\ \frac{\partial u_i}{\partial n} = \frac{\partial u_e}{\partial n} & \text{on } \Gamma_R. \end{cases} \quad (5.5)$$

Assume that we can solve for u_e analytically. We want to construct a map that relates $u_i|_{\Gamma}$ and $\frac{\partial u_i}{\partial n}|_{\Gamma}$. The next theorem is a standard theorem for trace mappings [3]

Theorem 5.1.1 *If $\partial\Omega$ is a smooth boundary of Ω then there are continuous (bounded) linear mappings (called traces)*

$$\tau : u \mapsto u|_{\partial\Omega} : H^k(\Omega) \mapsto H^{k-\frac{1}{2}}(\partial\Omega). \quad (5.6)$$

For our problem, the Hilbert space is $V := H^1(B_R)$ with the smooth boundary Γ_R . Hence, $u|_{\Gamma_R} \in H^{\frac{1}{2}}(\Gamma_R)$. We then define the map

$$T_R : H^{1/2}(\Gamma_R) \mapsto H^{-1/2}(\Gamma_R)$$

by

$$T_R(u_i|_{\Gamma_R}) = \frac{\partial u_i}{\partial n} \Big|_{\Gamma_R}. \quad (5.7)$$

Consequently, the boundary condition

$$\frac{\partial u_i}{\partial n} \Big|_{\Gamma_R} = \frac{\partial u_e}{\partial n} \Big|_{\Gamma_R}$$

becomes

$$T_R(u_i|_{\Gamma_R}) = \frac{\partial u_e}{\partial n} \Big|_{\Gamma_R}. \quad (5.8)$$

Before we construct T_R explicitly, we consider the following auxiliary problem in the exterior domain Ω_e :

Given $k^2 n_{cl}^2 < \beta^2$ and $g \in H^{-1/2}(\Gamma_R)$,

find $u_e \in H^1(\Omega_e)$ such that

$$\begin{cases} \Delta u_e + (k^2 n_{cl}^2 - \beta^2) u_e = 0 & \text{in } \Omega_e, \\ u_e = g & \text{on } \Gamma_R. \end{cases} \quad (5.9)$$

Lemma 5.1.2 *The auxiliary problem (5.9) has a unique solution $u_e \in H^1(\Omega_e)$.*

Proof: Let's set $w = u_e - \tilde{g}$ where

$$\tilde{g} = \begin{cases} g & \text{on } \Gamma_R \\ 0 & \text{elsewhere.} \end{cases}$$

Hence, $w \equiv 0$ on Γ_R . Hence, we obtain

$$\begin{cases} \Delta w + (k^2 n_{cl}^2 - \beta^2) w = 0 & \text{in } \Omega_e, \\ w = 0 & \text{on } \Gamma_R. \end{cases} \quad (5.10)$$

Let $H = L^2(\Omega_e)$ and $V = \{\omega \in H^1(\Omega_e) : \omega = 0 \text{ on } \Gamma_R\}$. Then $V \subset H$ is a Hilbert space. The variational formulation of (5.10) is

$$a(w, v) := \int_{\Omega_e} \nabla w \cdot \nabla v dx dy + (\beta^2 - k^2 n_{cl}^2) \int_{\Omega_e} w v dx dy.$$

Since $\beta^2 - k^2 n_{cl}^2 > 0$, $a(\cdot, \cdot)$ is coercive and bounded. By Lax-Milgram theorem, (5.10) has unique solution. This proves the lemma. ■

With this existence and uniqueness result, we can find the solution u_e in (5.9) explicitly. In polar coordinates, the exterior problem becomes

$$\begin{cases} \frac{\partial^2 u_e}{\partial r^2} + \frac{1}{r} \frac{\partial u_e}{\partial r} + \frac{1}{r^2} \frac{\partial^2 u_e}{\partial \theta^2} - (\beta^2 - k^2 n_{cl}^2) u_e = 0 & \text{in } \Omega_e \\ u_e|_{\Gamma_R} = g(\theta) & \text{on } \Gamma_R. \end{cases}$$

Using the Fourier series representation of u_e , i.e.,

$$u_e(r, \theta) = \sum_{m=0}^{\infty} u_e^{(n)}(r) e^{in\theta}, \quad (5.11)$$

we obtain

$$\frac{d^2 u_e^{(n)}}{dr^2} + \frac{1}{r} \frac{du_e^{(n)}}{dr} - \left[\frac{n^2}{r^2} + (\beta^2 - k^2 n_{cl}^2) \right] u_e^{(n)} = 0. \quad (5.12)$$

We denote

$$\alpha = \sqrt{\beta^2 - k^2 n_{cl}^2}.$$

For each $n = 1, 2, \dots$,

$$u_e^{(n)} = A_n K_n(\alpha r) + B_n I_n(\alpha r). \quad (5.13)$$

However, only $K_n(\alpha r)$ is an L^2 function. Thus

$$u_e(r, \theta) = \sum_{n=0}^{\infty} A_n K_n(\alpha r) e^{in\theta}. \quad (5.14)$$

On the boundary Γ_R , we also express the boundary function $g(\theta)$ in Fourier series, *i.e.*,

$$g(\theta) = \sum_{n=0}^{\infty} g^{(n)} e^{in\theta}. \quad (5.15)$$

Then, the condition $u_e = g$ on Γ_R yields

$$A_n K_n(\alpha R) = g^{(n)} \quad n = 0, 1, 2, \dots,$$

or

$$A_n = \frac{g^{(n)}}{K_n(\alpha R)}. \quad (5.16)$$

Therefore, the solution u_e is of the form

$$u_e = \sum_{n=0}^{\infty} \frac{g^{(n)}}{K_n(\alpha R)} \cdot K_n(\alpha r) e^{in\theta}. \quad (5.17)$$

We note that

$$\frac{\partial u_e}{\partial n} \Big|_{\Gamma_R} = \frac{\partial u_e}{\partial r} \Big|_{\Gamma_R} = \sum_{n=0}^{\infty} \alpha \frac{K'_n(\alpha R)}{R_n(\alpha R)} g^{(n)} e^{in\theta}. \quad (5.18)$$

Thus, we can define the map $T_R : H^{\frac{1}{2}}(\Gamma_R) \mapsto H^{-\frac{1}{2}}(\Gamma_R)$ as follows

$$\begin{aligned} T_R(\phi) &:= \sum_{n=0}^{\infty} \alpha \frac{K'_n(\alpha R)}{K_n(\alpha R)} \phi^{(n)} e^{in\theta} \\ &= \sum_{n=0}^{\infty} T_R^{(n)}(\phi) e^{in\theta}. \end{aligned}$$

In the next lemma, we study some of the properties of T_R .

Lemma 5.1.3 $T_R : H^{\frac{1}{2}}(\Gamma_R) \mapsto H^{-\frac{1}{2}}(\Gamma_R)$ defined by

$$T_R \phi = \sum_{n=0}^{\infty} \alpha \frac{K'_n(\alpha R)}{K_n(\alpha R)} \phi^{(n)} e^{in\theta}$$

is a continuous, symmetric, and linear operator.

Proof: The linearity of T_R is obvious. We note that if $\Psi \in H^{\frac{1}{2}}(\Gamma_R)$,

$$\begin{aligned} \langle T_R \phi, \Psi \rangle &:= \oint_{\Gamma_R} T_R \phi \cdot \bar{\Psi} d\Gamma_R \\ &= \int_0^{2\pi} \left(\sum_{n=0}^{\infty} T_R^{(n)}(\phi) e^{in\theta} \cdot \sum_{n=0}^{\infty} \bar{\Psi}^{(n)} e^{-in\theta} \right) R d\theta \\ &= 2\pi R \sum_{n=0}^{\infty} T_R^{(n)}(\phi) \bar{\Psi}^{(n)} \\ &= 2\pi R \sum_{n=0}^{\infty} \alpha \frac{K'_n(\alpha R)}{K_n(\alpha R)} \phi^{(n)} \bar{\Psi}^{(n)}. \end{aligned} \tag{5.19}$$

By the definition of dual norm, we have

$$\begin{aligned} \|T_R \phi\|_{H^{-\frac{1}{2}}(\Gamma_R)} &:= \sup_{\|\Psi\|_{H^{\frac{1}{2}}(\Gamma_R)}=1} |\langle T_R \phi, \Psi \rangle| \\ &\leq \sup_{\|\Psi\|_{H^{\frac{1}{2}}(\Gamma_R)}=1} 2\pi R \sum_{n=0}^{\infty} \alpha \left| \frac{K'_n(\alpha R)}{K_n(\alpha R)} \right| \cdot |\phi^{(n)}| \cdot |\Psi^{(n)}|. \end{aligned}$$

Since $K'_n(\alpha R) < 0$ and $K_n(\alpha R) > 0$, we can write

$$\left| \frac{K'_n(\alpha R)}{K_n(\alpha R)} \right| = \frac{-K'_n(\alpha R)}{K_n(\alpha R)}.$$

Using the following identity in [1]

$$zK'_n(z) = -nK_n(z) - zK_{n-1}(z),$$

we get

$$\begin{aligned} \frac{-K'_n(\alpha R)}{K_n(\alpha R)} &= \frac{n}{\alpha R} + \frac{K_{n-1}(\alpha R)}{K_n(\alpha R)} \\ &\leq \frac{n}{\alpha R} + 1. \end{aligned}$$

Thus, for sufficiently large n , we have

$$\frac{n}{\alpha R} + 1 \leq (n^2 + 1)^{1/2}.$$

In fact, the inequality holds for $n > 2\alpha R/(\alpha^2 R^2 - 1)$. Thus, for $n \gg 1$, we obtain

$$\sum_{n=0}^{\infty} \left| \frac{K'_n(\alpha R)}{K_n(\alpha R)} \right| \cdot |\phi^{(n)}|^2 \leq \sum_{n=0}^{\infty} (1 + n^2)^{\frac{1}{2}} \cdot |\phi^{(n)}|^2.$$

Hence, by Cauchy-Schwarz's inequality, we obtain

$$\sum_{n=0}^{\infty} \left| \frac{K'_n(\alpha R)}{K_n(\alpha R)} \right| \cdot |\phi^{(n)}| \cdot |\Psi^{(n)}| \leq \|\phi\|_{H^{\frac{1}{2}}(\Gamma_R)}.$$

So, T_R is bounded in $H^{1/2}(\Gamma_R)$. The symmetry of T_R is clear from definition. ■

Now, we are ready to define the interior problem.

(iii) *The interior problem in Ω*

Find $(\beta^2, u_i) \in R^* \times H^1(B_R) \setminus \{0\}$

$$(P_i) \quad \begin{cases} \Delta u_i + (k^2 n^2 - \beta^2) u_i = 0 & \text{in } B_R, \\ \frac{\partial u_i}{\partial n} \Big|_{\Gamma_R} = T_R(u_i|_{\Gamma_R}) & \text{on } \Gamma_R. \end{cases} \quad (5.20)$$

We need show that the new problem is equivalent to the original problem (P_0) .

Lemma 5.1.4 $(\beta^2, u) \in R^* \times H^1(\mathbb{R}^2) \setminus \{0\}$ is a solution of (P_0) iff $(\beta^2, u_i) \in R^* \times H^1(B_R) \setminus \{0\}$ is a solution of (P_i) .

Proof: Suppose (β^2, u) is a solution of (P_0) . Let $u_i := u|_{B_R}$. Then $u_i \neq 0$; otherwise, by the continuity conditions $u_e = u_i$ and $\frac{\partial u_e}{\partial n} = \frac{\partial u_i}{\partial n}$ on Γ_R , we would get $u_e|_{\Gamma_R} = 0$ and $\frac{\partial u_e}{\partial n}|_{\Gamma_R} = 0$. It would imply that $u_e \equiv 0$, so $u \equiv 0$. By the definition of T_R , we see that

$$\begin{aligned} T_R(u_i|_{\Gamma_R}) &= T_R(u_e|_{\Gamma_R}) \\ &= \frac{\partial u_e}{\partial n} \Big|_{\Gamma_R} \\ &= \frac{\partial u_i}{\partial n} \Big|_{\Gamma_R}. \end{aligned}$$

Thus $u|_{\Omega_i}$ also satisfies the boundary condition in (P_i) . Consequently, let (β^2, u_i) be a solution of (P_i) . Let u_e be the unique solution of the exterior domain with the fixed β^2 with boundary condition $u_e|_{\Gamma_R} = u_i|_{\Gamma_R}$. Hence, we see that

$$\frac{\partial u_i}{\partial n} \Big|_{\Gamma_R} = T_R(u_i|_{\Gamma_R}) = T_R(u_e|_{\Gamma_R}) = \frac{\partial u_e}{\partial n} \Big|_{\Gamma_R}.$$

Thus, $u_e|_{\Gamma_R} = u_i|_{\Gamma_R}$ and $\frac{\partial u_e}{\partial n} \Big|_{\Gamma_R} = \frac{\partial u_i}{\partial n} \Big|_{\Gamma_R}$ are satisfied. The function u whose restrictions on Ω_i and Ω_e are u_i and u_e is a solution of (P_0) . This u is unique because u_e is unique (by Lax-Milgram for the exterior problem). ■

5.2 Variational Formulation of Interior Problem

We recall that $H = L^2(B_R)$ is a Hilbert space with the usual inner product and L^2 -norm and $V := H^1(B_R) \subset H$ be a subspace. Let n_α be an arbitrary constant such that $n_\alpha > n_{co}$. The bilinear form $b(\cdot, \cdot)$ defined on $V \times V$ is

$$b(u, v) := \int_{B_R} \nabla u \cdot \nabla \bar{v} \, dx dy + k^2 \int_{B_R} (n_\alpha^2 - n^2) u \bar{v} \, dx dy - \oint_{\Gamma_R} T_R(u|_{\Gamma_R}) \bar{v} \, d\Gamma_R$$

$$\begin{aligned}
&= \int_{B_R} \nabla u \cdot \nabla \bar{v} \, dx dy + k^2 \int_{B_R} (n_\alpha^2 - n^2) u \bar{v} \, dx dy \\
&\quad + 2\pi R \sum_{n=0}^{\infty} -\alpha \frac{K'_n(\alpha R)}{K_n(\alpha R)} u^{(n)} \bar{v}^{(n)}. \tag{5.21}
\end{aligned}$$

Note that we have introduced the term $k^2 n_\alpha^2(u, v)$ into the variational form.

Lemma 5.2.1 *The bilinear form $b(\cdot, \cdot)$ is symmetric, bounded, and coercive, i.e., there exists $C_1, C_2 > 0$ such that*

$$|b(u, v)| \leq C_1 \|u\|_V \|v\|_V,$$

$$b(u, u) \geq C_2 \|u\|_V^2.$$

Proof: The symmetry of $b(u, v)$ follows from its definition, i.e.,

$$b(u, v) = \overline{b(v, u)}.$$

Since the linear map T_R is bounded in $H^{-\frac{1}{2}}(\Gamma_R)$, we have

$$\|T_R(u|_{\Gamma_R})\|_{H^{-1/2}(\Gamma_R)} \leq C \|u\|_{H^{1/2}(\Gamma_R)}.$$

Hence, by the Schwarz's inequality, we have

$$\begin{aligned}
\left| \oint_{\Gamma_R} T_R(u|_{\Gamma_R}) \bar{v} d\Gamma_R \right| &\leq C \|u\|_{H^{1/2}(\Gamma_R)} \|v\|_{H^{1/2}(\Gamma_R)} \\
&\leq C \|u\|_{H^1(B_R)} \|v\|_{H^1(B_R)}.
\end{aligned}$$

The last inequality follows from the trace theorem mentioned earlier. Thus, we have

$$\begin{aligned}
|b(u, v)| &\leq \|\nabla u\|_H \|\nabla v\|_H + k^2 (n_\alpha^2 - n_\alpha^2) \|u\|_H \|v\|_H + C \|u\|_V \|v\|_V \\
&\leq C \|u\|_V \|v\|_V.
\end{aligned}$$

Hence, $b(u, v)$ is bounded in $V \times V$. To show that $b(\cdot, \cdot)$, we notice that $-\frac{K'_n(\alpha R)}{K_n(\alpha R)} > 0$, we get

$$b(u, u) \geq \|\nabla u\|_H^2 + k^2(n_\alpha^2 - n^2)\|u\|_H^2 \geq C\|u\|_V^2.$$

Thus, $b(\cdot, \cdot) > 0$ for non-zero $u \in V$. ■

Lemma 5.2.2 *For each $f \in L^2(B_R)$, there is a unique solution $u \in V$ to the non-homogeneous variational equation*

$$b(u, v) = (f, v) \quad \forall v \in V. \quad (5.22)$$

Moreover, $u \in H^2(B_R)$ and

$$\|u\|_{H^2(B_R)} \leq C\|f\|_{L^2(B_R)}. \quad (5.23)$$

Proof: The existence and uniqueness of the solution $u \in V$ is the standard consequence of Lax-Milgram theorem. The regularity of u is also a standard result in potential theory [22] where the non-homogeneous problem is viewed equivalently as

$$\begin{cases} \Delta u_i + k^2(n_\alpha^2 - n^2)u_i = f & \text{in } B_R, \\ \Delta u_e + k^2(n_\alpha^2 - n_{cl}^2)u_e = 0 & \text{in } \mathbb{R}^2 \setminus B_R, \\ u_i = u_e & \text{on } \Gamma_R, \\ \frac{\partial u_i}{\partial n} = \frac{\partial u_e}{\partial n} & \text{on } \Gamma_R, \\ \sqrt{r} \frac{\partial u_e}{\partial r} \rightarrow 0, \sqrt{r} u_e \rightarrow 0 & \text{as } r \rightarrow \infty. \end{cases}$$

This completes the proof. ■

By a representation theorem for bounded symmetric bilinear forms, there exists a unique bounded self-adjoint operator B defined on $D(B) \subset V$ such that

$$b(u, v) = (Bu, v) \quad \forall u, v \in V.$$

and B has the same bounds as $b(\cdot, \cdot)$. Since 0 is a point in the resolvent set of B , the resolvent $T := B^{-1}$ is well-defined, i.e., T is bounded.

Lemma 5.2.3 *T is a compact operator in H .*

Proof: Since $H^1(B_r)$ is compactly embedded in $H = L^2(B_R)$,

$$T : H \mapsto D(B) \subset V = H^1(B_R) \hookrightarrow H.$$

Therefore, T is compact. ■

This implies that

Theorem 5.2.4 [20] *The spectrum of B consists of entirely of isolated eigenvalues with finite multiplicities and $R_\zeta(B) := (B - \zeta)^{-1}$ is compact for every ζ in the resolvent set of B .*

5.3 Finite Element Approximation

This section is very similar to section 4 in Chapter 4. Suppose that V_h is a family of finite dimensional subspaces of V that satisfies the approximation properties.

Approximation Properties of V_h : For any $u \in H^s(B_R)$, there exists an interpolant $\pi_h u \in V_h$ such that

$$\|u - \pi_h u\|_{H^l(B_R)} \leq Ch^{s-l} \|u\|_{H^s(B_R)}, \quad s \geq l, \quad (5.24)$$

where h is the mesh size. Since we mainly work with triangular linear elements, h is the maximum of the diameters of triangles in a triangulation.

As in Chapter 4, we first study the discrete inhomogeneous problem:

let $f \in H$, find $u_h \in V_h$ such that

$$b(u_h, v^h) = (f, v^h) \quad \forall v^h \in V_h.$$

Let $(B_h, D(B_h))$ be the unique self-adjoint operator associated to $b(\cdot, \cdot) : V_h \times V_h \mapsto \mathbb{C}$. Let $T_h := B_h^{-1}$. Then T_h is compact, in fact, T_h is of finite rank. Then a unique solution u_h to the inhomogeneous problem is of the form

$$u_h = T_h f, \quad f \in H. \quad (5.25)$$

We have the same convergence rate as in the singular Sturm-Liouville case, *i.e.*, theorem 4.5.4.

Theorem 5.3.1 *Let u and u_h be the unique solutions of the variational problems:*

$$b(u, v) = (f, v), \quad v \in V, \quad (5.26)$$

$$b(u_h, v^h) = (f, v^h), \quad v^h \in V_h. \quad (5.27)$$

Then they satisfy

$$\|u - u_h\|_V \leq Ch \|u\|_{H^2(B_R)}, \quad (5.28)$$

$$\|u - u_h\|_H \leq Ch^2 \|u\|_{H^2(B_R)}. \quad (5.29)$$

Proof: By Céa's lemma, we have

$$\begin{aligned} b(u - u_h, u - u_h)^{\frac{1}{2}} &\leq C \inf_{v^h \in V_h} b(u - v^h, u - v^h)^{\frac{1}{2}} \\ &\leq C \inf_{v^h \in V_h} \|u - v^h\|_V \\ &\leq C \|u - \pi_h u\|_V \\ &\leq Ch \|u\|_{H^2(B_R)}. \end{aligned} \quad (5.30)$$

But, we also have

$$b(u - u_h, u - u_h)^{\frac{1}{2}} \geq C \|u - u_h\|_V,$$

thus,

$$\|u - u_h\|_V \leq Ch\|u\|_{H^2(B_R)}.$$

Hence, the first inequality holds.

Now we use *Nitsche's trick* as follows. Let $g \in H$. Let $w_g \in H$ be the unique (dual) solution of

$$b(v, w_g) = (g, v), \quad v \in V.$$

Then we have

$$\begin{aligned} \inf_{w^h \in V_h} b(w_g - w^h, w_g - w^h)^{\frac{1}{2}} &\leq Cb(w_g - \pi_h w, w_g - \pi_h w)^{\frac{1}{2}} \\ &\leq C\|w_g - \pi_h w_g\|_V \\ &\leq Ch\|w_g\|_{H^2(B_R)} \\ &\leq Ch\|g\|_{L^2(B_R)}, \end{aligned}$$

therefore, $\|w_g - w^h\|_V \leq Ch\|g\|_{L^2(B_R)}$ for h sufficiently small. Thus, by *Aubin-Nitsche Lemma*, we get

$$\begin{aligned} \|u - u_h\|_H &\leq C\|u - u_h\|_V \left(\sup_{\|g\|_{L^2(B_R)}=1} \inf_{w^h \in V_h} \|w_g - w^h\|_V \right) \\ &\leq Ch^2\|u\|_{H^2(B_R)}. \end{aligned}$$

This proves the second inequality. ■

Corollary 5.3.2 *For $h > 0$ sufficiently small, we have*

$$\|T_h - T\| \leq Ch.$$

This corollary implies that the compact discrete operators T_h converges in norm to the compact operator T . Now we consider the variational form of eigenvalue problem:

$$\text{Find } (\lambda, u) \in \mathbb{R}^* \times V \text{ such that } b(u, v) = \lambda(u, v) \quad \forall v \in V \quad (5.31)$$

where $\lambda = k^2 n_\alpha^2 - \beta^2$. By the theorem 5.2.4 the eigenvalues λ are isolated since if μ is an eigenvalue of T then $\lambda = \frac{1}{\mu}$. This is important for numerical computations. The associated discrete eigenvalue problem is

$$\text{Find } (\lambda_h, u_h) \in \mathbb{R}^* \times V_h \text{ such that } b(u_h, v^h) = \lambda_h(u_h, v^h) \quad \forall v^h \in V_h. \quad (5.32)$$

We now state the standard theorem in finite element theory on the convergence rate of the eigenvalues and eigenvectors for the operator B with compact resolvent T .

Theorem 5.3.3 [12] *Let λ_0 be an isolated eigenvalue of B with a normalized eigenvector u_0 . Then there exists an eigenvalue λ_h of B_h with a normalized eigenvector u_h such that*

$$|\lambda_h - \lambda| \leq Ch^2$$

and

$$\|u_h - u\|_H \leq Ch.$$

5.4 Numerical Experiments

Now we present some numerical experiments of the finite element method.

Let us recall the variational form

$$b(u, v) = \int_{B_R} \nabla u \nabla v \, dx dy + \int_{B_R} k^2(n_\alpha^2 - n^2)uv \, dx dy - \oint_{\Gamma_R} T_R u \, v \, d\Gamma_R$$

where

$$T_R u = \sum_{n=0}^{\infty} \alpha \frac{K'_n(\alpha R)}{K_n(\alpha R)} u^{(n)} e^{in\theta}.$$

For computation, we rewrite the series expansion of the boundary operator T_R as

$$T_R u = \sum_{n=0}^{\infty} \alpha \frac{K'_n(\alpha R)}{K_n(\alpha R)} (u_1^{(n)}(R) \cos(n\theta) + u_2^{(n)}(R) \sin(n\theta))$$

where $u_1^{(n)}(r)$ and $u_2^{(n)}(r)$ are the Fourier coefficients of u defined as

$$\begin{aligned} u_1^{(0)}(r) &= \frac{1}{2\pi} \int_0^{2\pi} u(r, \theta) d\theta, \\ u_1^{(n)}(r) &= \frac{1}{\pi} \int_0^{2\pi} u(r, \theta) \cos(n\theta) d\theta, \quad \text{for } n \geq 1, \\ u_2^{(0)}(r) &= 0, \\ u_2^{(n)}(r) &= \int_0^{2\pi} u(r, \theta) \sin(n\theta) d\theta, \quad \text{for } n \geq 1. \end{aligned}$$

We define a triangulation \mathcal{T} in the bounded computational domain B_R as usual and the corresponding partition \mathcal{P} of the circle Γ_R . Let V_h be defined as

$$V_h := \{v^h \in V : v^h|_\tau \in P^1(\tau), \tau \in \mathcal{T}, v^h|_\gamma \in P^1(\gamma), \gamma \in \mathcal{P}\}. \quad (5.33)$$

We consider a step-index circular fiber with core radius $a = 1$, core refractive index $n_{co}^2 = 2$, and cladding index $n_{cl} = 1$. Let Γ_R be a the circle of radius $R = 2$. For the circular case, there exist exact analytical solutions in terms of Bessel functions $J_n(Ur)$ and modified Bessel functions $K_n(Wr)$ where

$$U = a\sqrt{k^2 n_{co}^2 - \beta^2}, \quad W = a\sqrt{\beta^2 - k^2 n_{cl}^2}$$

and the associated eigenvalue equations are [5]

$$\begin{aligned} \left(\frac{J'_n(U)}{U J_n(U)} + \frac{K'_n(W)}{W K_n(W)} \right) \left(\frac{n_{co}^2}{n_{cl}^2} \frac{J'_n(U)}{U J_n(U)} + \frac{K'_n(W)}{W K_n(W)} \right) \\ = n^2 \left(\frac{1}{U^2} + \frac{1}{W^2} \right) \left(\frac{n_{co}^2}{n_{cl}^2} \frac{1}{U^2} + \frac{1}{W^2} \right). \end{aligned} \quad (5.34)$$

Therefore, we can compare our results with the exact solutions. As we can see from the tables that with only coarse meshes we can obtain good approximations to the exact eigenvalues. The errors are about 5 %.

Table 5.1: FEM eigenvalues for $k^2 = 3.762625$

h	FEM	Error	Exact
.7789	2.216394		
.4203	2.253553	0.037159	
.2908	2.258267	0.004714	
.1137	2.258286	0.000019	2.2001

Table 5.2: FEM eigenvalues for $k^2 = 5.783529$

h	FEM	Error	Exact
.7789	2.904700		
.4203	2.953218	0.048518	
.2908	2.961140	0.007922	
.1137	2.965274	0.004134	
.0916	2.965319	0.000045	2.8930

5.5 Square Fiber Versus Circular Fiber

In this section, we apply the above method to compute the evanescent energy existing outside of a fiber. This energy is important in optical spectroscopy. The cladding of the fiber is removed. The core is then used as sensor.

We consider a square fiber of side $s = \sqrt{2}$ and a circular fiber of radius $a = \frac{\sqrt{2}}{2}$. The circular core is smaller than the square one. The evanescent energy of each mode excited in a fiber is the L^2 -norm of the solution restricted to the exterior region. Let $n_{cl} = 1$ for air and the core index $n_{co} = 1.5$. We will vary the wavelength λ and observe the change in the evanescent energy in each fiber. Since the lower order modes are dominant, we concentrate on the first two modes (LP_{01} and LP_{02}) which are always excited under a normal illumination. In the figures, we plot the whole intensity of the propagating modes over the computational domain and also the portion of the

evanescent intensity outside each fiber. We use the meshes with size $h = .1128$ for the square fiber and $h = .1137$ for the circular one. We observe that as the wavelength λ increases, more evanescent energy exists outside of each fiber. Though the square fiber is larger in core area, its evanescent energy is about twice as that of the circular fiber for both considered modes (LP_{01} , LP_{02}). The last figure shows the percentage of evanescent energy as a function of the wavelength $\lambda = 0.45\mu m, \dots, 2\mu m$. It is clear that the square fiber releases more evanescent energy to the outside region than the circular fiber. Hence, it seems that for spectroscopy application, square fibers would be a better tool.



Figure 5.1: LP_{01} mode in circular fiber, $\lambda = 1.6\mu m$



Figure 5.2: LP_{02} mode in circular fiber, $\lambda = 1.6\mu m$

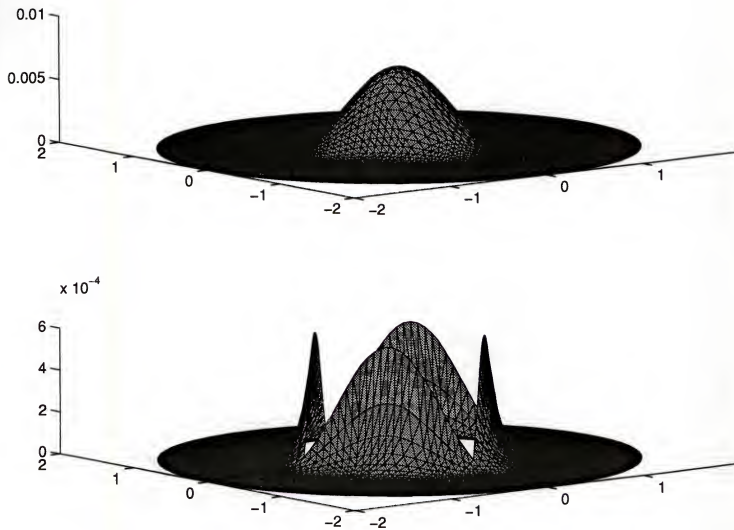


Figure 5.3: LP_{01} mode in square fiber, $\lambda = 1.2\mu m$

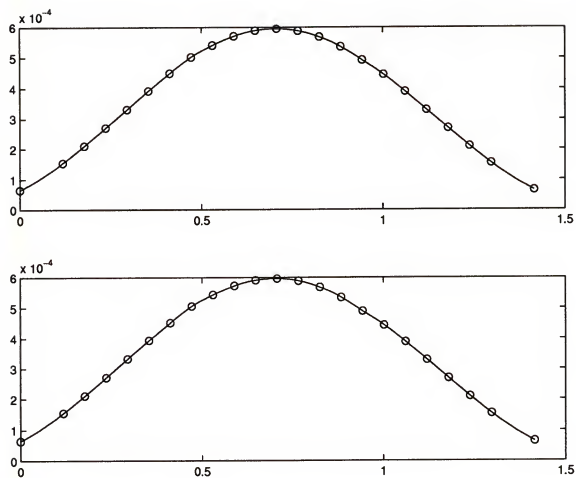


Figure 5.4: The profile of the evanescent intensity at the interface of LP_{01} mode in square fiber

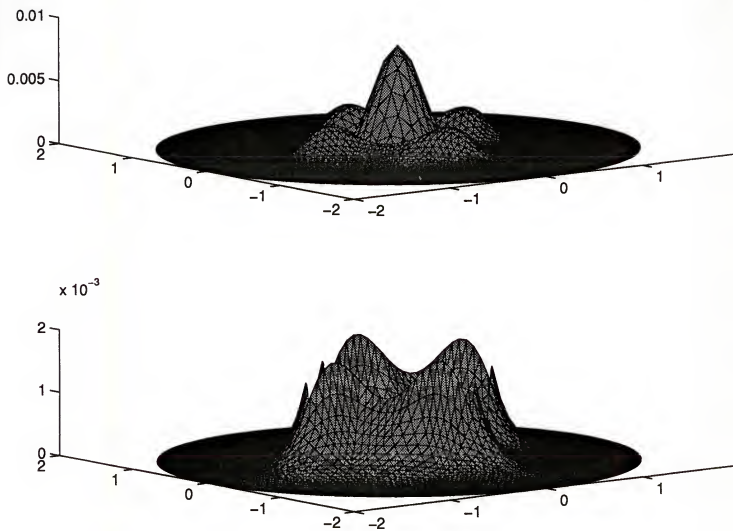


Figure 5.5: LP_{02} mode in square fiber, $\lambda = 1.2\mu m$

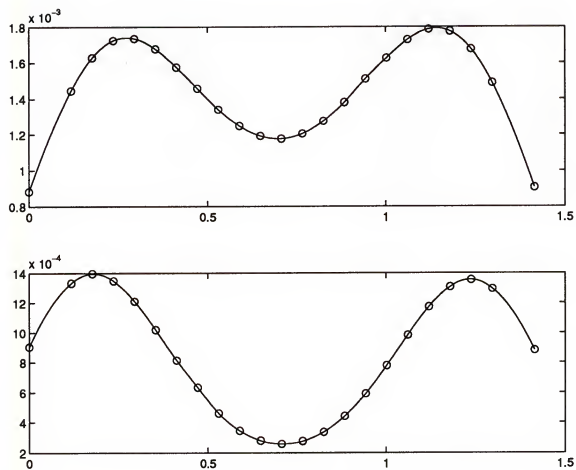


Figure 5.6: The profile of the evanescent intensity at the interface of LP_{02} in square fiber, $\lambda = 1.2\mu m$

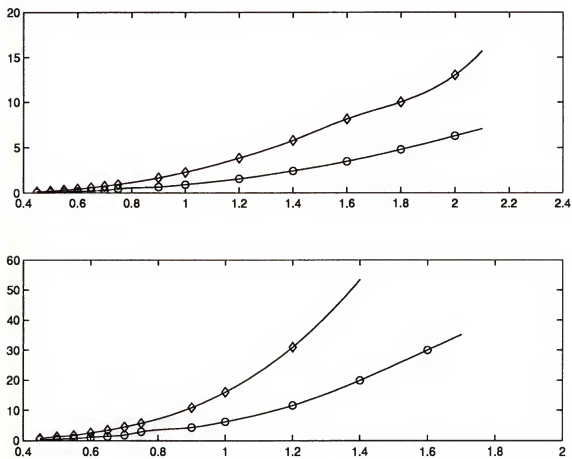


Figure 5.7: The evanescent energy vs λ . Circular:○, square:◻. Top: LP_{01} modes. Bottom: LP_{02} modes.

REFERENCES

- [1] M. Abramowitz and I.A. Stegun, *Handbook of Mathematical Functions*, Dover, New York, 1965.
- [2] R. Adams, *Sobolev Spaces*, Academic Press, New York, 1975.
- [3] I. Babuska and A. Aziz, *Survey lectures on the mathematical foundations of the finite element method* in A. Aziz (ed.): *The Mathematical Foundations of the Finite Element Method with Applications to Partial Differential Equations*, Academic Press, New York, 1972.
- [4] A. Bamberger and A.S. Bonnet, *Mathematical analysis of the guided modes of an optical fiber*, SIAM J. Math. Anal., Vol. **21**, no. 6 (1990), 1487-1510.
- [5] J. Buck, *Fundamentals of Optical Fibers*, John Wiley & Sons, Inc., New York, 1995.
- [6] P. Ciarlet, *The Finite Element Method for Elliptic Problems*, North-Holland, Amsterdam, 1978.
- [7] E.A. Coddington and N. Levinson, *Theory of Ordinary Differential Equations*, McGraw-Hill, New York, 1955.
- [8] L. Cowsar and T. Van, *A Finite element method for solving scalar wave equations*, preprint.
- [9] J.A. Cox and T. Van, *Bandwidths of the circular fibers*, preprint.
- [10] N. Dunfords and J.T. Schwartz, *Linear Operators*, Interscience Publishers, New York, I 1957, II 1963.
- [11] K. Eriksson and V. Thomee, *Garlerkin methods for singular boundary value problem in one space dimension*, Math.Comp., **42** 1984, 345-367.
- [12] G. Fix, *Eigenvalue approximation by the finite element method*, Advances in Math., **10** (1973), 300-316.
- [13] G. Fix and G. Strang, *An Analysis of The Finite Element Method*, Prentice Hall, New Jersey, 1973.
- [14] D. Givoli, *Numerical methods for problems in infinite domains*, Elsevier, Amsterdam, 1992.

- [15] D. Gloge and E.A.J. Marcatili, *Multimode theory of graded-core fibers*, B.S.T.J., Vol. **52**, no. 9 (1973), 1563-1578.
- [16] J.E. Goell, *A circular-harmonic computer analysis of rectangular dielectric waveguides*, B.S.T.J., 1969, 2133-2160.
- [17] W. H \ddot{o} hn, *Finite elements for the eigenvalue problem of the differential operators in unbounded domain*, Math. Meth. in the Appl.Sci., **7** (1985), 1-39.
- [18] D. Jespersen, *Ritz-Galerkin methods for singular boundary value problems*, SIAM J.Num.Anal., **15** (1978), 813-834.
- [19] P. Joly and C. Poirier, *A numerical method for the computation of electromagnetic modes in optical fibers*, Rapport de rechercher, INRIA, no. 2974 (1996).
- [20] T. Kato, *Perturbation Theory for Linear Operators*, Springer-Verlag, New York, 1976.
- [21] A. Kufner, *Weighted Sobolev Spaces*, John Wiley and Sons, New York, 1985.
- [22] R.C. MacCamy and S.P. Marin, *A finite element method for exterior interface problems*, Internat. J. Math. & Math. Sci., vol.**3**, no.2 (1980), 311-350.
- [23] E.A.J. Marcatili, *Dielectric rectangular waveguide and directional coupler for integrated optics*, B.S.T.J., 1969, 2071-2102.
- [24] D. Marcuse, *Calculation of bandwidth from index profiles of optical fibers. 1: Theory*, Applied Optics, **18** (1979), 2073-2080.
- [25] D. Marcuse, H.M. Presby, and L.G. Cohen, *Calculation of bandwidth from index profiles of optical fibers. 2: Experiments*, Applied Optics, **18** (1979), 3249-3255.
- [26] D. Marcuse and H.M. Presby, *Effects of profile deformations on fiber bandwidth*, Applied Optics, **18** (1979), 3758-3763.
- [27] W. Mills, *Optimal error estimates for the finite element spectral approximation of non-compact operators*, SIAM J.Numer.Anal., **16** (1979), 704-718.
- [28] P.M. Morse and H. Feshbach, *Methods of Theoretical Physics*, McGraw-Hill, New York, 1953.
- [29] E. Muller-Pfeiffer, *Spectral theory of Ordinary Differential Operators*, Ellis Horwood, Chichester, 1981.
- [30] R. Olshansky, *Pulse broadening caused by deviations from the optimal index profile*, Applied Optics, **15** (1975), 782-788.
- [31] J. Rappaz, *Approximation of the spectrum of a non-compact operator given by the magnetohydrodynamic stability of a plasma*, Num.Math., **28** (1977), 15-24.
- [32] A.W. Snyder and J.D. Love, *Optical Waveguide Theory*, Chapman-Hall, London, 1983.

- [33] E.T. Whittaker and G.N. Watson, *A Course of Modern Analysis*, Cambridge University Press, London, 1952.
- [34] R. Yamada and Y. Inabe, *Guided waves in an optical square-law medium*, Journal of The Optical Society of America **64** (1974), 964-968.

BIOGRAPHICAL SKETCH

Tri Van was born in Saigon, South Vietnam, on September 11, 1970. He escaped the Communists to Malaysia by boat in the summer of 1986. After six months in the refugee camp, he arrived in Gainesville, Florida in February 1987 to live with his uncle, Phong Huynh. A year later, his brother, Ton Van, also escaped to Thailand and joined him in Gainesville in 1988. He graduated from Gainesville High School in May 1988 and went to New College in Sarasota, Florida. In the fall semester of 1990, he attended the Budapest Semesters in Mathematics at Eötvös University, Budapest, Hungary. In 1991, his father and his sister, Tien Van, were allowed to leave Vietnam to come to America. In 1992, he received a Bachelor of Arts degree in Mathematics, then moved to Long Island, New York to attend State University of New York, Stony Brook, New York. Finally, in 1993, he saw his mother for the first time since he left her eight years ago. He finished a Master of Arts degree in Mathematics/Applied Mathematics in 1994. In July 1999, he becomes an American citizen.

I certify that I have read this study and that in my opinion it conforms to acceptable standards of scholarly presentation and is fully adequate, in scope and quality, as a dissertation for the degree of Doctor of Philosophy.



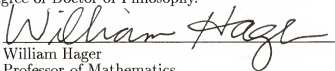
Gang Bao , Chairman
Associate Professor of Mathematics

I certify that I have read this study and that in my opinion it conforms to acceptable standards of scholarly presentation and is fully adequate, in scope and quality, as a dissertation for the degree of Doctor of Philosophy.



Lawrence Cowsar
Member of Technical Staff, Lucent Technologies

I certify that I have read this study and that in my opinion it conforms to acceptable standards of scholarly presentation and is fully adequate, in scope and quality, as a dissertation for the degree of Doctor of Philosophy.



William Hager
Professor of Mathematics

I certify that I have read this study and that in my opinion it conforms to acceptable standards of scholarly presentation and is fully adequate, in scope and quality, as a dissertation for the degree of Doctor of Philosophy.



Li-Chien Shen
Professor of Mathematics

I certify that I have read this study and that in my opinion it conforms to acceptable standards of scholarly presentation and is fully adequate, in scope and quality, as a dissertation for the degree of Doctor of Philosophy.



Weihong Tan
Assistant Professor of Chemistry

This dissertation was submitted to the Graduate Faculty of the Department of Mathematics in the College of Liberal Arts and Sciences and to the Graduate School and was accepted as partial fulfillment of the requirements for the degree of Doctor of Philosophy.

August 1999

Dean, Graduate School